MOLECULAR MECHANISMS OF TAY SACHS DISEASE: CALCIUM, EXCITOTOXICITY, AND APOPTOSIS

By

John-Paul A.C. King, B.Sc. (Honours)

A Thesis
Submitted to the School of Graduate Studies
in Partial Fulfillment of the Requirements
for the Degree
Master of Science

McMaster University

MASTER OF SCIENCE (2007)
(Biology)

McMaster University
Hamilton, Ontario

TITLE: Molecular mechanisms of Tay Sachs Disease: calcium, excitotoxicity, and apoptosis

AUTHOR: John-Paul A.C. King, B.Sc. (Honours), Memorial University

SUPERVISOR: Suleiman A. Igdoura, Ph.D., Associate Professor, McMaster University

NUMBER OF PAGES: xiv, 77

Abstract

The objective is to investigate the molecular mechanisms leading to neurodegeneration in Tay Sachs disease, a lysosomal storage disorder caused by a deficiency in the enzyme hexosaminidase A. This was accomplished using microarray analysis of normal and Tay Sachs neuroglia. Microarray data analysis was performed using Onto Express, PANTHER software, and cluster analysis. The expression levels of selected genes were validated using Real Time PCR. To establish a physiological relationship between G_{M2} accumulation and the expression of these genes, their expression was assessed after treatment with an inhibitor of ganglioside synthesis, n-butyldeoxynojirimycin (NBDNJ). Neuronal pentraxin 1 (NPTX1), potassium channel, subfamily K, member 2 (KCNK2), and prostaglandin synthase 1 (PTGS1) were found to be upregulated in Tay Sachs neuroglia while heme oxygenase (HMOX1) was downregulated. The mRNA levels of NPTX1, KCNK2, PTGS1, and HMOX1 all reverted to normal levels in response to ganglioside synthesis inhibitor. Pentraxin RNA levels were also reduced in response to sialidase overexpression, another method of GM2 reduction. Pentraxin protein levels were also increased in Tay Sachs cells in response to α-amino-3-hydroxy-5-methylisoxazole-4- propionic acid (AMPA), and were attenuated upon treatment with either NBDNJ or AMPA antagonist 2,3-dihydroxy-6-nitro-7-sulfamoyl-benzo [f]quinoxaline-2,3-dione (NBQX). Strong colocalization was seen between NPTX1 and the AMPA receptor as well as the glutamate transporter EAAC1. AMPA receptor function was also enhanced as illustrated by an increase in calcium influx upon stimulation. This stimulation also resulted in increased apoptosis during

AMPA receptor stimulation. In this study, our genetic profiling experiment led to the identification of NPTX1 as a marker of pathogenesis in Tay Sachs Cells. The role of NPTX1 in excitotoxicity implicates the latter in disease mechanism associated with Tay Sachs disease. Furthermore, this study provides evidence that TSD cells undergo programmed cell death in response to increased intracellular calcium as a result of increased glutamate receptor stimulation.

ACKNOWLEDGEMENTS:

To my supervisor, Dr. Suleiman Igdoura, thank you for everything you have done for me. Your support, guidance, and work ethic have, and will continue to be an inspiration for me, and will never be forgotten. Your sense of humor made it a peleaseure to show up to the lab every day. Thank you also to Dr. Dino Trigatti. Your expertise and advice made every experiment better than the previous one and I am proud to have worked with you. To my committee members, thank you for reviewing this thesis and providing assistance when it was most needed.

To the members of the Igdoura lab, past and present, thank you for your support and friendship. To Taryne, I cannot thank you enough for your friendship. You made the days where nothing worked still seem like good days. To Marc, who kept me in shape, helped with experiments I didn't understand, and made sure I walked away every day smiling, I cannot thank you enough. To Katie, you have helped me through the most difficult time of my life. What you mean to me cannot be measured. I will cherish what we have forever. To Pat Hayward, you have always gone above and beyond your duties to make sure the graduate students of McMaster Biology are taken care of, myself included. You are an inspiration and I would not have been able to do this without your help.

To my family and friends, thank you for all you have done for me. Thank you to all those who helped make Hamilton a home; John and Denny for being fathers when I could not be with mine, Debbie and Cherie for being mothers. Thank you to Jessica and Kevin, for your friendship and hospitality all this time. To my mother, who has always

guided me, who taught me how to live righteously. Most of all, this is for you dad. I wish you were here with me, and I know that I have made you proud.

TABLE OF CONTENTS:

CHAPTER 4: DICUSSION

LIST OF FIGURES:

LIST OF TABLES:

LIST OF ABBREVIATIONS:

AIDS	Acquired Immunodeficiency Syndrome
AMPA	α-amino-3-hydroxy-5-methyl-4-isoxazolepropionic acid
ARHGDIA	Rho GDP Dissociation Inhibitor Alpha
ATP	Adenosine Triphosphate
BCIP	5-Bromo-4-chloro-3-indolyl phosphate
cDNA	Complementary Deoxyribonucleic Acid
CASP	Caspase
CAPN	Calpain
CBE	conduritol b-epoxide
CCD	Charged Coupled Device
CNS	Central Nervous System
cRNA	Complementary Ribonucleic Acid
CTP	Cytosine Triphosphate
CRP	C-Reactive Protein
DMEM	Dulbecco's modified Eagle's medium
DNA	Deoxyribonucleic Acid
dNTP	Deoxynucleotide Triphosphate
EDTA	ethylenediamine tetraacetic acid
EAAC	Excitatory Amino Acid Carrier
EAAT	Excitatory Amino Acid Transporter
EGFR	Endothelial Growth Factor Receptor
ER	Endoplasmic Reticulum
FBS	Fetal Bovine Serum
FITC	Fluorescein Isothiocyanate
GLUR	Guanosine Receptor
GTP	Adenosine Triphosphate
HEXA	Hexosaminidase A
HEXB	Hexosaminidase B
HDAC	Histone Deacetylase
HMOX	Heme Oxygenase
IL	Interleukin
ITPR3	Inositol Triphosphate Receptor
KCNK2	Potassium Channel, Subfamily K, Member 2
MAPK	Mitogen-Activated Protein Kinase
MOI	Mode of Infection
MRP	Mitochondrial ribosomal protein
mRNA	messenger Ribonucleic Acid
NBDNJ	N-butyldeoxynojirimycin
NBT	Nitro Blue Tetrazolium
NBQX	2,3-dihydroxy-6-nitro-7-sulfamoyl-benzo[f]quinoxaline-2,3-dione
NMDA	N-methyl-D-aspartate

NPTX	Neuronal Pentraxin
PAGE	Polyacrylamide gel electrophoresis
PANTHER	Protein Analysis Through Evolutionary Relationships
PBS	Phosphate Buffered Saline
PCR	Polymerase Chain Reaction
PDGF	Platelet Derived Growth Factor
PKA	Protein Kinase A
PKC	Protein Kinase C
PLCB	Phospholipase C Beta
PMT	Photomultiplier
PTGS	Prostaglandin Synthase
RNA	Ribonucleic Acid
RT-PCR	Reverse Transcriptase Polymerase Chain Reaction
SAP	Serum Amyloid Protein
SERCA	Sarco/Endoplasmic Reticulum Ca^{2+}-ATPase
SDS	Sodium Dodecyl Sulfate
SMPD	Sphingomyelin Phosphodiesterase
STAT	Signal Transducer and Activator of Transcription
TdT	Terminal Deoxynucleotidyl Transferase
TSD	Tay Sachs Disease
TTP	Thymidine Triphosphate
UDP	Uridine Diphosphate
UTP	Uridine Triphosphate

CONTRIBUTIONS:

Thank you to Dr. Colin Nurse for equipment and help with the Calcium Imaging experiment.

1 Introduction

1.1 Gangliosides

Gangliosides are a subclass of glycosphingolipids; membrane bound molecules containing ceramide, the lipid anchor, with a variable carbohydrate side chain facing the extracellular space. Inclusion of sialic acid in the carbohydrate moiety differentiates the gangliosides from the other classes of glycosphingolipids. Members of the family include GM1, GM2, GD1a, and GD1b, designated and differentiated by the number of sialic acid residues contained in the carbohydrate chain. It is this carbohydrate portion of the molecule that confers functional specificity of individual ganglioside; a feature greatly influenced by the negatively charged sialic acid, or neuraminic acid, residue.

Gangliosides are multifunctional molecules that are involved in numerous cellular processes such as signal transduction (Spiegel et al., 1996), vascular smooth muscle cell proliferation (Gouni-Berthold et al., 2001), neuron outgrowth (Walkley et al., 1998) and neuronal survival (Ferrari and Greene, 1998). In addition, gangliosides have been shown to indirectly regulate gene expression. For instance, GM3 accumulation via overexpression of GM3 synthase has been shown to reduce PDGFα receptor mRNA levels (Inokuchi et al, 2006). However, little has been reported on a possible correlation between ganglioside accumulation and changes in gene expression.

1.2 Ganglioside catabolism

Like other membrane-bound molecules, these are turned over through endocytosis. GM1, which is typically on the cell surface, is internalized, (Taki et al., 1981) and broken down to GM2 in the lysosome via the action of β-galactosidase. Normal catabolism of GM2 ganglioside then requires three gene products: the α and β subunits of β-hexosaminidase A, and the GM2 activator protein. The gene, *hexa*, encodes the α-subunit of the protein while the *hexb* gene encodes for the β-subunit. The HEXA protein is a heterodimer of an α and a β peptide while HEXB is a homodimer of the β polypeptide. Once internalized as part of the plasma membrane, the activator protein binds to GM2 to expose the sugar moieties for hydrolysis. HEXA can then bind to GM2 and cleave the terminal N-acetylglucosamine, yielding GM3 (Gravel, 2001). Specific lysosomal enzymes continue to cleave other sugars from the molecule in a stepwise fashion until fatty acid and sphingosine are obtained.

1.3 Ganglioside Storage Disorders

Mutations in any of the genes coding for the peptides involved in catabolism interrupts the pathway, resulting in one of several lysosomal storage disorders. Dysfunction of the HEXB leads to Sandhoff disease while inactivation of HEXA gives rise to Tay Sachs disease; A mutation in the gene coding for the GM2 activator will cause the AB variant known as G_{M2} activator deficiency (Meier et al., 1991). These diseases are

collectively called GM2 gangliosidosis and are characterized by an accumulation of GM2 ganglioside in the lysosomes of neural tissue which eventually lead to cell death, neurodegeneration and death.

Although a reduction in the enzyme activity is the cause of the disease, one has to consider the notion that the absence of the functional gene product is only indirectly responsible for the neurodegeneration. Disease mechanisms such as neuroinflammation, apoptosis, complement activation, or ER stress are major contributors to the CNS damage in GM2 gangliosidosis patients (Yam et al., 2006). It has been shown that accumulation of gangliosides in the ER membrane in GM1 gangliosidosis interferes with the calcium-rectifying channel in the ER preventing the recovery of an ER stress response (d'Azzo et al, 2006). This illustrates the potential effect that accumulating gangliosides have on the function of cellular proteins revealing potentially new therapeutic targets.

1.4 Mouse models

Mice with a defective *hexa* or *hexb* gene have been produced, thereby providing a model for both Tay Sachs and Sandhoff disease (Phaneuf et al., 1996;Sango et al., 1995). The Sandhoff mouse ($hexb^{-/-}$) experiences a rapid and progressively fatal neuronal degeneration in a similar fashion as the human disease. Although biochemically, the murine and human HEXA deficiencies are somewhat similar, they are phenotypically different. In the Tay Sachs disease mouse ($hexa^{-/-}$) GM2 levels are maintained at non-

toxic levels thereby escaping the neurological effects associated with the human disease (Phaneuf et al., 1996). This phenomenon is mediated by a compensatory biological process involving lysosomal sialidase, which converts GM2 to GA2 bypassing the requirement for the *hexa* gene product. The two β subunits of HEXA form Hexosaminidase-B and can then catalyze the conversion of GA2 to GM3 and continue subsequently via other enzymes thereby circumventing the disease (Igdoura et al., 1999).

1.5 Inflammation

Inflammation is a hallmark of neurodegenerative diseases such as the lysosomal storage disorders. It is impossible to examine the process of neuroinflammation without discussing the microglia. As resident CNS cells, microglia are functionally equivalent to macrophages. Once activated, they are recruited to sites of neuronal injury where they participate in phagocytosis of dead cells and other debris. Activation of microglia coincides with CNS infiltration of polymorphonuclear leukocytes from the blood to remove antigens and to aid in tissue repair (Diamond et al. 1999). Various proinflammatory factors including cell adhesion molecules, interleukin 1, interleukin 3, interleukin 6, tumor necrosis factor, tumor growth factor, and colony stimulating factor are produced by the activated glia (Hays 1998; Wu et al. 1998; Kim et al. 2001; Sun et al. 2004a; Drew et al. 2005; Minghetti et al. 2005; Noda et al. 2006). Complement proteins are also secreted by not only microglia but also astrocytes, neurons, and oligodendrocytes (Hosokawa et al. 2003).

Problems occur, however, when this inflammation response becomes chronic, as is seen in several neurodegenerative disorders such as Alzheimer's, Parkinson's and Tay Sachs disease (Eikelenboom et al., 1991; Hirsch et al., 1998; Jeyakumar et al., 2003). Even though the multitude of inflammatory factors secreted during neural trauma are in place to repair damage, prolonged exposure of these cytokines leads to chronic inflammation, a process thought to be deleterious. Although it is not clearly established, some believe that this prolonged response is responsible for inducing apoptosis in the CNS and inhibition of this response is the focus of much research. However, it is still unclear how lysosomal accumulation results in a chronic inflammation response. As insightful as it would be, there is little information regarding the transcriptional activity that translates GM2 accumulation in the lysosome to a chronic inflammatory and subsequent neurodegenerative response. This information is crucial to discovering other pathways that may be involved in inducing inflammation and apoptosis in neurodegenerative disorders.

1.6 Therapy

Sialidase is a lysosomal enzyme that catalyzes the removal of sialic acid residues from hexose or hexosamine molecules. The normal conversion of GM3 to lactosylceramide is accomplished by this enzyme. It requires the association of a multi-enzyme complex of sialidase, β-galactosidase, and a protective protein cathepsin A, (d'Azzo et al., 1982). In addition to its catabolic function, the complex can also act as a

signaling molecule during the activation of macrophage activating factor T-lymphocytes (Stamatos et al., 2003). In the *hexa*$^{-/-}$ mouse, the murine sialidase can convert GM2 to GA2 glycolipid (Riboni et al., 2004). The GA2 can then be reduced to a lactosylceramide molecule. Therefore, the mouse model of alpha subunit deficiency (Tay Sachs disease) can still catabolize GM2 molecules with the aid of a lower affinity Hexosaminidase-B enzyme. This process however, does not appear to occur at a significant rate in human cells and may be due to differences in substrate specificity, enzyme concentrations, or differences in sialidase dependant inflammatory mechanisms.

Efforts have been made to replicate the sialidase bypass in human Tay Sachs cells. Neuroglia cells from a human Tay Sachs patient were transfected with human sialidase cDNA to upregulate the peptide expression and cull the accumulation of GM2 in the lysosomes (Igdoura et al., 1999). The experiment was successful in reducing the GM2 concentration in the cells. This offers evidence that the amount of sialidase leads to the GM2 to lac-ceraminde bypass but does not rule out the possibility of varied affinities between the murine and human enzymes being responsible for this phenotypic difference.

Substrate deprivation therapy has also shown promising results in reducing the accumulation of GM2. N-butyldeoxynojirimycin (NBDNJ) was originally utilized as a potential AIDS treatment since it interferes with viral replication, albeit via an unknown mechanism (Karpas et al., 1988). Further studies, however, identified the compound as an inhibitor of UDP-glucose ceramide glucosyltransferase, responsible for the addition of glucose to the ceramide molecule in the first step of gangliosides synthesis (Platt et al.,

1994). Consequently, treatment with this glucose analogue has proven to be a viable means to reduce levels of accumulated gangliosides in several lysosomal storage disorders. Treatment resulted in reduction of several characteristics associated with *hexb*$^{-/-}$ mice including reduction in accumulated GM2 in the CNS as well as periphery tissues, alleviation of paralysis, increased lifespan, and abolishment of apoptosis of the neurons (Jeyakumar et al., 1999). Although the *hexa-/-* Tay Sachs mouse model show no neurodegenerative features, the GM2 accumulation associated with the animals are reduced when treated with NBDNJ (Platt et al., 1997). Niemann-Pick type C disease, although not associated with a ganglioside metabolism mutation, is also associated with an accumulation of GM2, GM3, and other glycosphingolipids, as well as neurological dysfunction resembling other lysosomal storage disorders. Mouse models of Niemann-Pick type C disease and Fabry's Disease (another ganglioside storage disorder) show delayed onset of neurological dysfunction, increased average life span and a reduction of ganglioside accumulation upon treatment with NBDNJ (Platt et. al., 2000). Finally, treatment of Gaucher HL-60 cells with NBDNJ shows a ninety percent reduction of glycolipid accumulation (Platt et al., 1994). After successful in vivo studies, clinical trials of NBDNJ have revealed a reduction in gangliosides accumulation in the liver and spleens of Gaucher patients (Cox et al., 2000).

1.7 Calcium, glutamate and excitotoxicity

The huge calcium concentration gradient between the extracellular space and the intracellular environment (mM and sub μM) provides a situation for calcium as a key mediator of intracellular signaling. Changes in membrane permeability allow for calcium influx and activation of several proteins residing in an environment which is normally relatively calcium-free. Maintaining conditions so different from the extracellular environment requires an intricate system of ion channels and intracellular calcium binding proteins, along with channels that allow influx of calcium in response to appropriate stimuli. In neurons, the former role is done by multiple plasma membrane proteins: an ATPase, an outwardly rectifying calcium channel, and a sodium-calcium antiporter. The latter role is provided by stimulatory ion channels, which provide synaptic transmission by using the calcium influx as an initiator of membrane depolarization and, subsequently, an action potential (Carafoli, 1987). One such mechanism is initiated by the release of glutamate from the presynaptic neuron followed by the binding of this excitatory amino acid to specific receptors on the postsynaptic neuron.

Glutamate mediates synaptic transmission by activation of 3 receptor families classified and named based on their responsiveness to glutamate analogues, NMDA (N-methyl-D-aspartate), AMPA (α-amino-3-hydroxy-5-methyl-4-isoxazolepropionic acid), and kainate (Kerkut et. al., 1974). These receptors are responsible for the long-term plasticity of the CNS, thought to be the underlying mechanism of learning and memory. Normal neuronal function involves release of glutamate into the synapse and subsequent

activation of the glutamate receptors, thereby inducing movement of cations and propagating the action potential. The AMPA receptor is a tetramer composed of combinations of one or more GLUR1-4. Although all of these channels are sodium permeable, lack of a GLUR2 subunit confers calcium permeability (Boulter et. al., 1990). Overstimulation of these receptors through deleterious mechanisms such as ischemic injury leads to apoptosis and is termed, excitotoxicity. The mechanism of excitotoxicity is believed to be via release of ER calcium stores since previous study has shown that not only does stimulation of glutamate receptors lead to increased expression of Bip, Chop, and caspase-12, but inhibition of ER-stress with salubrinal protects against apoptosis via glutamate (Sokka et. al., 2007). While the neuroprotective effects of gangliosides are well documented, there is evidence that they may enhance susceptibility of cells to excitotoxicity since GM1 administration increases the expression of NMDA receptors in the brain of rats (Liu et al., 2005).

Excitotoxicity has been suggested to be one of the major underlying mechanisms involved in neurodegeneration associated with Alzheimer's (Dickey et al, 2003), Huntington's (Cha et al, 1998), as well as Ischemia (Colbourne et al, 2003). Upon release of glutamate into the synapse, transporters remove the amino acid from the extracellular space to reduce the stimulus and thereby prevent excitotoxicity. This role is undertaken by the Excitatory Amino Acid Transporters EAAT1-5, also termed Excitatory Amino Acid Carriers (EAAC's), the glutamate transporters. Improper regulation of these neuron and glia resident proteins can also lead to excitotoxicity and neurodegeneration (Smith et al, 1994).

The EAAT/EAAC glutamate transporters play a vital role in the reduction of excitotoxicity. At the synaptic cleft, the EAAT's exchange glutamate, a hydrogen ion, and 3 sodium ions for 1 potassium ion (Zerangue and Kavanaugh 1996). The glutamate is subsequently processed through the glutamate-glutamine cycle and transported back to the excitatory neuron. Here, it is converted back into glutamate and once again used as a neurotransmitter (Benjamin and Quastel 1975). Although astrocytes provide the major contribution to EAAT mediated glutamate removal, microglia, oligodendrites, and the neurons themselves may also contribute (Danbolt, 2001).

Another equally important mechanism for controlling the glutamate response in neurons is the trafficking and clustering these receptors on the cell surface. One protein involved in this mechanism is neuronal pentraxin 1 (NPTX1). NPTX1 colocalizes with and aids in the clustering of GLUR1-2 receptors to the cell membrane at the synapse. Pentraxin is upregulated in the presence of the glutamate analogue AMPA (alpha-amino-3-hydroxy-5-methyl-4-isoxazolepropionic acid) and initiates an apoptotic response which is NPTX1-dependant (Hossain et al., 2004). Another group focusing on pentraxin showed that potassium deprivation has the same effect on pentraxin and apoptosis (DeGregorio-Rocasolano et al., 2001), although a connection between these pathways remains unknown.

2 Methods and Materials

2.1 Materials

Rabbit Anti-Mouse IgG + IgM (H+L) antibody (315-005-044) was obtained from Jackson ImmunoResearch Laboratories, Inc. Anti-NPTX1 mouse antibody (610369) was purchased from BD Transduction Laboratories. Rabbit anti-EAAC1 antibody was purchased from Chemicon. All other primary antibodies were acquired from Santa Cruz (anti-NPTX1 antibody from Santa Cruz, sc-12122; anti-GLUR1 from Santa Cruz: sc-13152). Secondary antibodies were as follows: EAAC1: anti-rabbit texas red; GLUR1, anti-mouse alexa 594; NPTX1, anti-goat FITC). Protein-A agarose for immunprecipitation was obtained from BioRad (153-6153). Promix [^{35}S]cysteine/methionine for radio-labeling was purchased from Amersham.

2.2 Microarray Analysis

Total RNA was isolated from Tay Sachs and Normal neuroglia using the RNEasy kit (Qiagen, #74104). 350 μL of Buffer RLT and 250 μL of 100% ethanol were added to the cells. The lysate was applied to an RNeasy spin column in a 2mL collection tube and centrifuged for 15 seconds at 8,000 X g. Two washes of 500 μL Buffer RPE were added to the columns and centrifuged at 8,000 X g for 15 seconds. The spin column was centrifuged at maximum speed for 2 minutes to dry the column. In a clean, 1.5mL collection tube, 50 μL of nuclease-free H_2O was added onto the membrane. Each column was incubated at ambient temperature for 10 minutes and then centrifuged for 1 minute at 8,000 X g. 2 μg of total RNA was combined with 2 μL of bacterial control working

solution. 1 µL of the T7 Oligo Primer was added, and the total volume was adjusted to 12 µL. Samples were incubated for 10 minutes at 70°C and placed on ice for 5 minutes. Each reaction was then combined with 2 µL 10X first strand buffer, 4 µL 5mM dNTP Mix, 1 µL RNase inhibitor, and 1 µL reverse transcriptase. The samples were then Incubated for 2 hours at 42 ^{O}C. 63 µL Nuclease-free H2O, 10 µL 10X Second Strand Buffer, 4 µL 5mM dNTP Mix, 2 µL DNA Polymerase, and 1 µL RNase H were then added to each tube and incubated for 2 hours at 16 ^{O}C. A QIAquick purification kit (Qiagen, # 28104) was used to purify the cDNA. 500 µL of buffer PB were added to the cDNA and added to a QIAquick spin column in a 2mL collection tube. Tubes were then centrifuged at 10,000 X g for 60 seconds. 700 µL of buffer PE was added to the column and centrifuged at 10,000 X g for 60 seconds. The column was centrifuged at 10,000 X g for 1 minute to dry the column. 30 µL of nuclease-free H_2O was then added to the center of the membrane, left for 1 minute, then centrifuged for 1 minute at 10,000 X g. this was the repeated with another 30 µL of H_2O and the elutant was dried in a SpeedVac under medium heat for 1 hour. Each cDNA sample was then combined with 9.5 µL nuclease-free H_2O and 4.0 µL 10X T7 Reaction Buffer, 4.0 µL T7 ATP Solution, 4.0 µL T7 CTP Solution, 4.0 µL T7 GTP Solution, 3.0 µL T7 UTP Solution, 7.5 µL 10mM Biotin-11-UTP, and 4.0 µL 10X T7 Enzyme Mix. Samples were then incubated for 14 hours at 37 ^{O}C. 60 µL of nuclease-free water was added to each reaction and purified using an RNeasy Mini Kit. 10 µg of cRNA was adjusted to a final volume of 20 µL with nuclease-free H2O in a PCR tube. 5 µL of 5X Fragmentation Buffer was added to each sample and heated for 20 minutes at 94 °C and put on ice for 5 minutes. The fragmented cRNA was

transferred to a clean 1.5 mL microcentrifuge tube and combined with 75 µL Hybridization Buffer Component A, and 125 µL Hybridization Buffer component B, 25 µL Nuclease-free H_2O. The solution was vortexed for 5 seconds at maximum speed, incubated at 90 °C for 5 minutes and cooled on ice for 5 minutes. 250 µL of the cRNA was injected into each slide port, sealed, and agitated at 300 rpm for 18 hours at 37 °C. 240mL of filtered 0.75 TNT Buffer (1X TNT Buffer: 1L 1M Tris-HCL, pH7.6, 300 mL 5M NaCl, 5mL Tween 20, 8.7L DI H_2O) was placed in a 46°C water bath overnight. The slides were then left in 0.75X TNT at room temperature for 10 minutes and the hybrdidization chambers were removed from the slides. Slides were then incubated in 0.75 X TNT for 1 hour at 46 °C. The rack of slides was then incubated in Cy 5 Streptavidin for 30 minutes at room temperature. The rack was then washed 4 times in 1X TNT at room temperature in the dark then dipped 5 times each in two successive solutions of 0.05% Tween 20. Slides were rinsed with ddH_2O, air dried for 3 minutes, and scanned at 635nm, PMT voltage of 600V with a resolution of 10 microns.

2.3 Cell Culture:

Neuroglia were cultured in high-glucose (4.5 mg/L) Dulbecco's modified Eagle's medium (DMEM) supplemented with 10 percent fetal bovine serum (FBS), 50 µg/mL penicillin, 50 µg/mL streptomycin, and 10 µg/mL amphotericin B. Cells were grown in 10 cm dishes, unless specified otherwise, at a density of approximately 90,000 cells per cm^2. The culture environment was at 37°C, 95% humidity, in the presence of 5% CO_2. Cells were lifted prior to seeding plates for experiments by adding 0.05% trypsin in 0.53

mM EDTA·4Na (Invitrogen, 25300054), 1 mL per 10 cm dish. Trypsin was removed after 1 minute of mild agitation and cells were resuspended in fresh media.

2.4 Real Time PCR

RNA from normal and Tay Sachs neuroglia was extracted using the RNEasy kit from Qiagen, as previously described. For each sample, 1 μg of RNA was mixed with 1 μl of 100 μM oligo$(dT)_{20}$ (Mobix), 2 μl 10 mM dNTP Mix (10 mM each dATP, dGTP, dCTP and dTTP at neutral pH) and sterile, distilled water to 13 μl. The mixture was heated to 65°C for 5 minutes and incubated on ice for 1 minute. To each tube, 4 μl 5X First-Strand Buffer, 1 μl 0.1 M DTT, 1 μl RNaseOUT™ Recombinant RNase Inhibitor (Invitrogen, 10777-019), 1 μl of SuperScript™ III RT was added, mixed and briefly centrifuged. Tubes were incubated at 50°C for 90 minutes and then inactivated by heating at 70°C for 15 minutes. Real-Time PCR was then done using as well as SYBR Green (Applied Bios stems, 4367659) in a 96 well plate. Each well contained 10 μl SYBR Green, 1 μl cDNA, 0.4 μl forward primers, 0.4 μl reverse primer, and 8.2 μl ddH_2O. β-actin primers were purchased from Applied Biosystems (401846) while all other primers were designed using PerlPrimer (see table 1). A standard curve for each gene was created using a dilution series (undiluted, 1:2, 1:4, 1:8 and 1:16) of the cDNA, in duplicate, from a sample of TSD cells. Each well of unknown concentration was completed in triplicate. Analysis of the reaction was completed using an ABI Prism 7900HT with SDS version 2.0 software.

Table 1: Primers used for Real Time PCR

Gene Name	Forward Primer (5'-3')	Reverse Primer (5'-3')
NPTX1	AGCAAGATCGATGAGCTG	TGTCTTTCTGACCTTTCTCG
CASP1	AAGTCGGCAGAGATTTATCC	TTTCACATCTACGCTGTACC
IL6	AAGTCGGCAGAGAATTATCC	TGCATCTAGATTCTTTGCCT
HMOX1	TCAACATCCAGCTCTTTGAG	AGAAAGCTGAGTGTAAAGAC
EOTAXIN	CACCTGCTGCTTTAACCT	GTTTGGTCTTGAAGATCACAG
KCNK2	AGCCTCATGAGATTTCACAG	CCTATGGTTATAACAGTGC
ITPR3	CTTCTTCTACCCTTACATGGAG	TCTTGTTGGTCAGATTGAGG
HDAC1	GAAGTCCGAGGCATCTG	CCCGATATCCCGTAGGT
PTGS1	CCTCTTTCACCCACTTCC	CTGCTTCTTCCCTTTGGT
SMPD1	GGCTGAAGAAGGAACCC	TCAAAGAGGTGGACAATGG
PLCB4	CTGGCTCACTACTTCATCAG	TCAACACATCTGCAACCA
CAPN1	CATCAGCAAACACAAAGACC	GCATCTCGTAGGCACTC
MRPL11	GCAAACAGGGAAAGAGGT	GGACAACAGACGACAGG
MRPS18A	ACTATGACGATGTTCTGCTG	ATTTGGTAATAGACCTGCTCG
ARHGDIA	GAGAGCTTCAAGAAGCAGTC	TCAGTCTTGTCAATCTTGACG

In brief, for each reaction, the cycle number (C_i) which yielded the inflection point on the curve of fluorescence versus cycle number was recorded. The dilution series was used to create a linear curve of concentration (undiluted having a value of 100; no units) versus (C_i). All subsequent readings of (C_i) were then plotted and used to extrapolate the relative concentration of each sample. To normalize, the relative concentration for each gene of each sample was divided by its corresponding relative against β-actin. Graphs were generated using Microsoft Excel.

2.5 Immunoprecipitation

Cells were seeded as previously described and washed with PBS and incubated for four hours in cysteine/methionine-free media containing 25 μCi/mL Promix ([^{35}S]cysteine/methionine). Cell lysate was collected with two 500 μL washes of immunoprecipitation buffer (10 mM sodium phosphate, 100 mM NaCl, 1% Triton X-100) and incubated with 1μL Rabbit Anti-Mouse IgG + IgM (H+L) for 30 minutes. Samples were centrifuged for 5 minutes at 800 x g and supernatant was incubated with antibody again for 1 hour at 4 °C. 0.5 μL anti-NPTX1 anti-mouse antibody was then added and tubes were rocked overnight at 4 °C. Protein-A agarose slurry (10 μL) was added and samples were incubated for another hour. Tubes were centrifuged again and pellets were washed 3 times with 1 mL of wash buffer (1% Triton X-100, 0.1% SDS, 150mM NaCl, 2mM EDTA, pH 8.0, 20mM Tris-HCl, pH 8.0). Pellets were dissolved in 40 μL Laemmli buffer (4% SDS, 20% glycerol, 10% 2-mercaptoethanol, 0.004% bromphenol blue, 0.125 M Tris HCl) and 20 μL was run on an 8% SDS-PAGE gel. Gels were then fixed with 45

% methanol, 10 % acetic acid, and 45 % H2O for 1 hour, incubated with Amplify™ (Amersham, NAMP100) for 1 hour, and washed in ddH_2O for 30 minutes. Gels were dried for 1 hour at 85 °C under vacuum and exposed with Hyperfilm (Amersham, 28-9068-36) for 8 hours.

2.6 Apoptosis determination

Cells were grown and seeded in a 24 well plate. After 24 hours of growth, cells were washed twice with cold PBS and fixed in 1% paraformaldehyde in PBS, pH 7.4 for 10 minutes at room temperature. Cells were then washed in 2 changes of PBS for 5 minutes each wash and permeabilized in precooled ethanol:acetic acid 2:1 for 5 minutes at -20 °C. Cells were washed again in 2 changes of PBS for 5 minutes each. Excess liquid was carefully aspirated from the specimen and equilibration buffer was immediately applied directly on the specimen at a concentration of 75 µL/5 cm2. Excess liquid was once again carefully aspirated from the specimen and working Strength TdT Enzyme (3:7 TdT Enzyme: Reaction Buffer) was added to each coverslip at a concentration of 55 µL/5 cm2. The plate was then incubated in a humidified chamber at 37°C for 1 hour.1 mL of Stop/Wash Buffer (1:35 stop/wash buffer concentrate:ddH_2O) was added to each well, agitated for 15 seconds and incubated for 10 minutes at ambient temperature. Alkaline phosphatase conjugated anti-digoxigenin was added 1:500 to PBS, warmed to room temperature, and added to each well at 65 µL/5 cm^2. Samples were incubated at ambient temperature for 1hour. Cells were washed again in 3 changes of PBS for 5 minutes each and 200 µL NBT/BCIP (1:50 stock solution : 0.1 M Tris-HCl, pH 9.5, 0.1 M NaCl) was

added to each well and incubated in a humidified chamber at room temperature overnight. Specimen were washed in changes of ddH_2O for 1 minute and counterstain in 0.5% (w:v) methyl green for 10 minutes at room temperature. Samples were then washed with agitation in 3 changes of ddH_2O for 1 minute each wash. Specimens were destained in 3 changes of 100% N-butanol in the same fashion. Coverslips were then mounted on slides using Aquamount (Fisher Scientific, NC9839881), dried at 45 °C for 1 hour, and viewed with an inverted light microscope.

Apoptotic cells were identified as cells with positive NBT/BCIP staining (very dark blue/black nuclei). 3 fields of view at 100X magnification were quantified for total cells (those staining for methyl green and NBT/BCIP) as well as apoptotic cells (NBT/BCIP only). Values for 3 fields were summated and expressed as apoptotic cells divided by total number of cells multiplied by 100.

2.7 Immunocytochemistry

Tay Sachs neuroglia were grown overnight on coverslips in a 24-well plate at a density of 90,000 cells per cm^2. Media was removed and washed twice with PBS and fixed with fresh 3.5% formaldehyde in PBS for 30 minutes at 37 °C. coverslips were washed with cold PBS for 5 minutes and incubated in 200 µL of 0.5% Triton X-100 in PBS for 30 minutes at room temperature. Cells were washed with cold PBS for 5 minutes and incubated in 5% fat-free milk in PBS for 1 hour at ambient temperature. Primary antibody was mixed with 5% milk in PBS at 1:200 and added to each well overnight at

$4^{O}C$. Wells were washed 4 times for 5 minutes with 0.025% Tween 20 in PBS and secondary antibody (1:200 in 5% milk in PBS) was added. Coverslips were mounted onto slides using Aquamount (Fisher Scientific, NC9839881), dried for 45 minutes, and viewed with an inverted microscope.

2.8 Calcium imaging

Cells were visualized on a Nikon Eclipse TE2000-U inverted microscope using a Nikon S-Fluor 40x oil immersion objective. Cells were maintained at 37°C and at pH 7.4 by perfusing with warmed, bicarbonate-buffered saline solution aerated with 5% CO_2/95% air mixture (PO_2 = 160 mmHg). Saline solution contained 24 mM $NaHCO_3$, 155 mM NaCl, 10 mM glucose, 12 mM sucrose, 5 mM KCl, 2 mM $CaCl_2$, 1 mM $MgCl_2$. Cells were loaded with 5 μM fura-2/AM, a fluorescent Ca^{2+} indicator, for 3-10 minutes, and subsequently washed for 15 minutes to remove free dye. The ratio of calcium-bound to calcium-unbound fura-2 was determined by monitoring the fluorescence intensity by exciting at 340 nm versus 380 nm.

Changes in $[Ca^{2+}]_i$ were indicated from changes in the fluorescence emitted at 510 nm as a result of alternate excitation at 340 nm and 380 nm. A Xenon light source was used to send UV light of different excitation wavelengths to the lambda DG-4 high-speed optical filter changer. Filtered light passed through the objective to the specimen, and light emitted by the specimen was passed through a fura-2 emissions filter cube to the Hamamatsu OCRCA-ET charge coupled device (CCD) camera. The CCD camera took 2 images every 2 seconds (one each at 340nm and 380nm, separated by a 200 ns interval). Intracellular calcium levels were monitored using simple PCI software version 5.3

(Compix), which displayed the ratio of fluorescence at 340 nm/380 nm throughout the experiment.

3 Results

3.1 Tay Sachs neuroglia show altered gene expression

To investigate differences in global gene expression between Tay Sachs and normal cells, a Codelink 20,000 gene microarray analysis was performed. Gene expression values from the Tay Sachs sample correlated strongly with the normal cells, yielding a correlation coefficient of 0.95. The technical duplicates showed reproducibility yielding correlation coefficients of 0.99 and 0.997 for the technical duplicates of TSD and normal cells respectively. Of the 20,000 genes examined, 4751 showed an expression difference greater than 1.5 fold between the two samples and 987 showed an expression difference greater than two-fold between normal and TSD samples.

To recognize and group genes with similar expression levels, a GeneScript cluster analysis was performed. The data revealed a greater number of upregulated genes compared to downregulated genes in the Tay Sachs cells (figure 1, table 2 and 3). Our gene profiling experiment revealed results highlighting physiological differences due to the disease. The Onto-Express Analysis in appendix A shows alterations of several genes involved in important biological pathways such as immune response, electron transport, neurogenesis, and apoptosis. Further analysis using PANTHER (appendix A, table 1) shows significant alteration in more specific pathways such as Inflammation, Interleukin signaling, Oxidative stress, and the glutamate receptor pathway.

Based on these findings, genes involved in several of these pathways were selected for validation using quantitative RT-PCR. To determine an appropriate control for the real time analysis, four housekeeping genes at different expression levels were examined, namely, β-actin, mitochondrial ribosomal protein S18A (MRPS18A), mitochondrial ribosomal protein L11 (MRPL11) and Rho GDP dissociation inhibitor alpha (ARHGDIA). RNA from normal and TSD cells was reverse transcribed and real time PCR was performed for each gene. Using biological triplicates, all four genes showed equal expression levels in the two cell types (see figure 2). As a result, all real time PCR experiments performed after that were normalized to β-actin.

Genes involved in pathways possibly related to the Tay Sachs phenotype were selected for investigation using real time PCR. Inflammatory factors such as Interleukin 6 (IL6), Prostaglandin synthase 1 (PTGS1), Eotaxin, Heme oxygenase 1(HMOX1) Histone Deacetylase 1 (HDAC1), and Caspase 1 (CASP1) were examined. Factors involved in calcium homeostasis including phospholipase C beta 4 (PLCB4), Calpain (CAPN1), and Inositol Triphosphate Receptor, Type 3 (ITPR3) were also tested. Sphingomyelin Phosphodiesterase 1 (SMPD1) was selected since it is involved in glycoshphingolipid regulation. Finally, Neuronal Pentraxin 1 and Potassium Channel, Subfamily K, Member 2 (KCNK2) are involved in ion balance and excitotoxicity. Figure 3 shows the expression levels of these genes using real time PCR. Neuronal Pentraxin 1, Interleukin 6, HMOX1, HDAC1, PTGS1, and KCNK2 show a difference in expression between Tay Sachs and Normal cells. CAPN1, Eotaxin, ITPR3, Caspase 1, PLCB4, and SMPD showed no significant difference between the two genotypes.

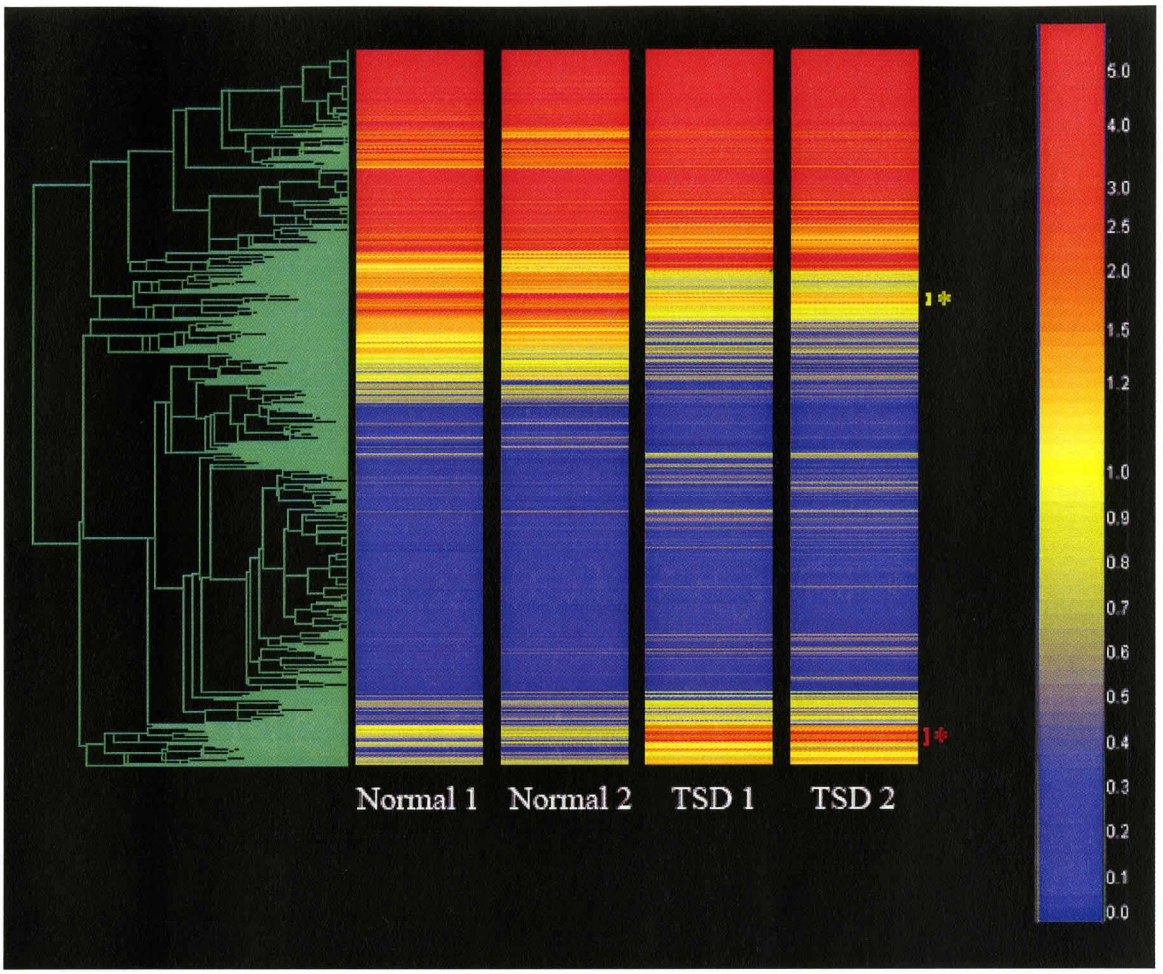

Figure 1: Gene expression levels are different between Tay Sachs cells and Normal cells. 20,000 genes were examined from two samples of TSD and Normal neuroglia cells. Out of these genes, 4751 were found to have an expression value difference of 1.5 fold or greater. These genes were analyzed using cluster analysis of log2 of expression. Genes with similar expression dynamics across all 4 samples were grouped together. In comparison to the Normals, the most downregulated genes in Tay Sachs cells are represented by a yellow asterisk, while the red asterisk illustrates genes with the highest upregulation.

Table 2: Genes that show highest upregulation in the Tay Sachs cells based on cluster analysis. Genes were selected from the region enclosed by the red line in figure 1.

Accession number	Gene Name	Normal 1	Normal 2	TSD 1	TSD 2	Average fold change
X56196	Xist, Coding Sequence 'D' (Locus DXS399E)."	0.112649	0.112864	23.74809	24.25321	212.8544
NM_018937	Protocadherin Beta 3 (PCDHB3)	0.116127	0.108617	0.639686	38.67695	174.94
NM_031957	Keratin Associated Protein 1.5 (KRTAP1.5)	0.385343	0.518996	16.29314	13.80315	33.27986
NM_002522	Neuronal Pentraxin I (NPTX1)	0.393272	0.512256	9.25377	9.324052	20.516
NM_004753	Short-Chain Dehydrogenase 1 (SDR1)	0.318276	0.310823	4.969836	5.157819	16.09867
NM_001453	Forkhead Box F2 (FOXF2)	0.077028	0.178126	1.451976	1.178614	10.30978
NM_000927	Atp-Binding Cassette, Sub-Family B (ABCB1)	0.190339	0.171489	1.536906	1.460533	8.284168
NM_003178	Synapsin Ii (SYN2)	0.243207	0.274271	0.17333	4.111601	8.280419
NM_014217	Potassium Channel K, Member 2 (KCNK2)	0.397483	0.487684	3.329749	3.588416	7.815662
NM_007063	Vascular Rab-Gap (VRP)	0.251998	0.306539	1.926298	2.098962	7.206796
NM_002338	Limbic System-Associated Membrane Protein (LSAMP)	0.793611	0.545548	4.546312	4.05161	6.42039
NM_002867	Rab3b, Member Ras Oncogene Family (RAB3B)	0.141078	0.157818	0.940119	0.878707	6.085153
NM_004617	Transmembrane 4, Member 4 (TM4SF4)	0.163522	0.203776	1.041853	1.020082	5.613787
NM_003004	Secreted And Transmembrane 1 (SECTM1)	0.465872	0.532201	2.917663	2.638268	5.566663
NM_002280	Keratin, Hair, Acidic, 5 (KRTHA5)	0.251146	0.237675	1.382476	1.321053	5.530707
NM_014181	Hspc159 (HSPC159)	0.188362	0.230051	1.041471	1.058387	5.018627
NM_000214	Jagged 1 (JAG1)	0.204414	0.217379	0.84112	0.935031	4.210957
NM_016186	Serine Proteinase Inhibitor 10 (SERPINA10)	0.221073	0.20209	0.949656	0.78694	4.103845
NM_003761	Vesicle-Associated Membrane Protein 8 (VAMP8)	0.219096	0.228394	0.947203	0.761803	3.819095
NM_002153	Hydroxysteroid Dehydrogenase 2 (HSD17B2)	0.40762	0.542421	1.853004	1.750345	3.792833
NM_031437	Norel Protein (NOREL)	0.389215	0.453768	1.539476	1.623021	3.751554
NM_021151	Carnitine O-Octanoyltransferase (CROT)	0.613853	0.421016	1.88517	1.96362	3.71911
NM_016428	Nesh Protein (NESH)	0.390922	0.494687	1.656509	1.581327	3.656054
NM_004170	Solute Carrier Family 1, Member 1 (SLC1A1)	0.531924	0.556254	1.838537	2.136342	3.652785
NM_031920	Arg99 Protein (ARG99)	0.373218	0.415462	1.271186	1.172629	3.098612
NM_013989	Deiodinase, Iodothyronine,	0.62925	0.732352	1.976787	2.103168	2.996437

	Type Ii (DIO2)					
NM_004000	Chitinase 3 (CHI3L2)	0.425315	0.531924	1.375857	1.485171	2.988832
NM_006209	Ectonucleotide Pyrophosphatase 2 (ENPP2)	0.364215	0.405125	1.076448	0.976472	2.668416
NM_002217	Pre-Alpha Inhibitor, H3 Polypeptide (ITIH3)	0.639395	0.604941	1.707561	1.611228	2.667116
NM_005397	Podocalyxin-Like (PODXL)	0.440325	0.43944	1.163632	1.108525	2.582688
NM_006829	Adipose Specific 2 (APM2)	0.923702	0.459665	1.719582	1.840537	2.573517
NM_001146	Angiopoietin 1 (ANGPT1)	0.406198	0.47745	1.13121	1.140205	2.570496
NM_004114	Fibroblast Growth Factor 13 (FGF13)	0.386686	0.458157	1.103461	1.009975	2.501571
NM_002924	Regulator Of G-Protein Signalling 7 (RGS7)	0.324331	0.432479	1.055631	0.822184	2.481225
NM_005308	G Protein-Coupled Receptor Kinase (GPRK5)	0.765989	0.920369	2.148255	1.989714	2.453791
NM_012124	Cysteine And Histidine-Rich Domain (CHORDC1)	0.973781	0.794803	2.016485	2.197002	2.382407
NM_003020	Secretory Granule Neuro-endocrine Protein (SGNE1)	0.669061	0.397562	1.242459	1.261072	2.347156
NM_005025	Serine Proteinase Inhibitor, Member 1 (SERPINI1)	0.774119	0.379191	1.13872	1.547032	2.328734
NM_015641	Testis Derived Transcript (TES)	0.616848	0.64463	1.571724	1.360226	2.324218
NM_014592	Kv Channel Interacting Protein 2 (KCNIP2)	0.111795	0.170258	0.154341	0.478154	2.242469
NM_003655	Chromobox Homolog 4 (CBX4)	0.691088	0.819212	1.823502	1.559572	2.240001
NM_000710	Bradykinin Receptor (Bdkrb1)	0.429649	0.424412	0.875309	1.032983	2.234372
NM_002449	Msh Homeo Box Homolog 2 (Drosophila) (MSX2)	0.600582	0.504521	1.25277	1.207474	2.226256
NM_006439	Collectin Sub-Family Member 10 (COLEC10)	0.036436	0.095828	0.135307	0.158931	2.224628
NM_001116	Adenylate Cyclase 9 (ADCY9)	0.452302	0.531924	1.103015	1.062029	2.199743
NM_006052	Down Syndrome Critical Region Gene 3 (DSCR3)	0.519716	0.394441	0.996048	1.005059	2.189021
NM_033035	Thymic Stromal Lymphopoietin (TSLP),	0.806096	0.813455	1.65206	1.866956	2.172835
NM_015899	Putative Glycolipid Transfer Protein	0.489855	0.506916	0.695063	1.435749	2.137714
NM_001531	Major Histocompatibility Complex (HLALS)	0.437114	0.455683	0.976132	0.910706	2.113402
NM_004165	Ras-Related Associated With Diabetes (RRAD)	1.208058	0.523302	1.925641	1.703817	2.096304
NM_004226	Serine/Threonine Kinase 17b (STK17B)	0.744313	0.434357	1.175888	1.257747	2.06473
NM_000038	Adenomatosis Polyposis Coli (APC)	0.703789	0.80426	1.545304	1.506127	2.023431
NM_020326	Atp-Binding Cassette, Member 4 (ABCD4),	0.580183	0.44176	1.032776	1.020481	2.009171

Table 2: Genes that show highest downregulation in the Tay Sachs cells based on cluster analysis. Genes were selected from the region enclosed by the yellow line in figure 1.

Accession number	Gene Name	Normal 1	Normal 2	TSD 1	TSD 2	Average fold change
NM_004660	Dead/H Box Polypeptide, Y Chromosome (Dby)	3.929387	2.566162	0.084477	0.163062	-26.2405
NM_004681	Eukaryotic Translation Initiation Factor 1a, Y Chromosome (Eif1ay)	2.954101	3.089427	0.199217	0.126845	-18.5349
NM_000337	Sarcoglycan, Delta (Sgcd)	3.254264	4.285355	0.23421	0.212342	-16.8841
AJ271372	Putative Bk(Ca) Channel Beta4 Subunit (Kcnmb4gene).	1.779416	2.139365	0.2229	0.246142	-8.35485
NM_006623	Phosphoglycerate Dehydrogenase (Phgdh)	2.1123	2.357561	0.346351	0.314834	-6.76038
NM_005822	Down Syndrome Critical Region Gene (Dscr1l1)	1.553065	1.824368	0.438946	0.43942	-3.84513
NM_002847	Protein Tyrosine Phosphatase, Receptor Type, N Polypeptide 2 (Ptprn2)	1.760385	1.277051	0.355134	0.463359	-3.71101
NM_006979	Hla Class Ii Region Expressed Gene Ke4 (Hke4)	1.514129	1.710053	0.46562	0.478255	-3.4159
NM_006455	Nucleolar Autoantigen (Sc65)	1.537745	1.672583	0.483822	0.537305	-3.14391
NM_000041	Apolipoprotein E (Apoe)	1.428922	1.620217	0.430488	0.568826	-3.05123
NM_016022	Cgi-78 Protein (Loc51107)	1.199756	1.5371	0.446819	0.452454	-3.04341
NM_020190	Hnoel-Iso Protein (Hnoel-Iso)	1.213748	1.436368	0.470457	0.450326	-2.87811
NM_017797	Btb (Poz) Domain Containing 2 (Btbd2)	1.224002	1.477676	0.519331	0.48435	-2.69177
NM_000455	Serine/Threonine Kinase 11 (Stk11)	1.500707	1.289502	0.53862	0.565905	-2.52616
NM_001933	Dihydrolipoamide S-Succinyltransferase (Dlst)	1.206002	1.368813	0.530953	0.525868	-2.43638
NM_001493	Gdp Dissociation Inhibitor 1 (Gdi1)	1.234531	1.402435	0.56292	0.626475	-2.21706
NM_015945	Ovarian Cancer Overexpressed 1 (Ovcov1)	1.296403	1.366323	0.629949	0.610254	-2.14701
NM_002613	3-Phosphoinositide Dependent Protein Kinase-1 (Pdpk1)	1.287043	1.470571	0.680488	0.619379	-2.12146
NM_014938	Mlx Interactor (Mondoa)	1.188324	1.478639	0.705021	0.619496	-2.01354

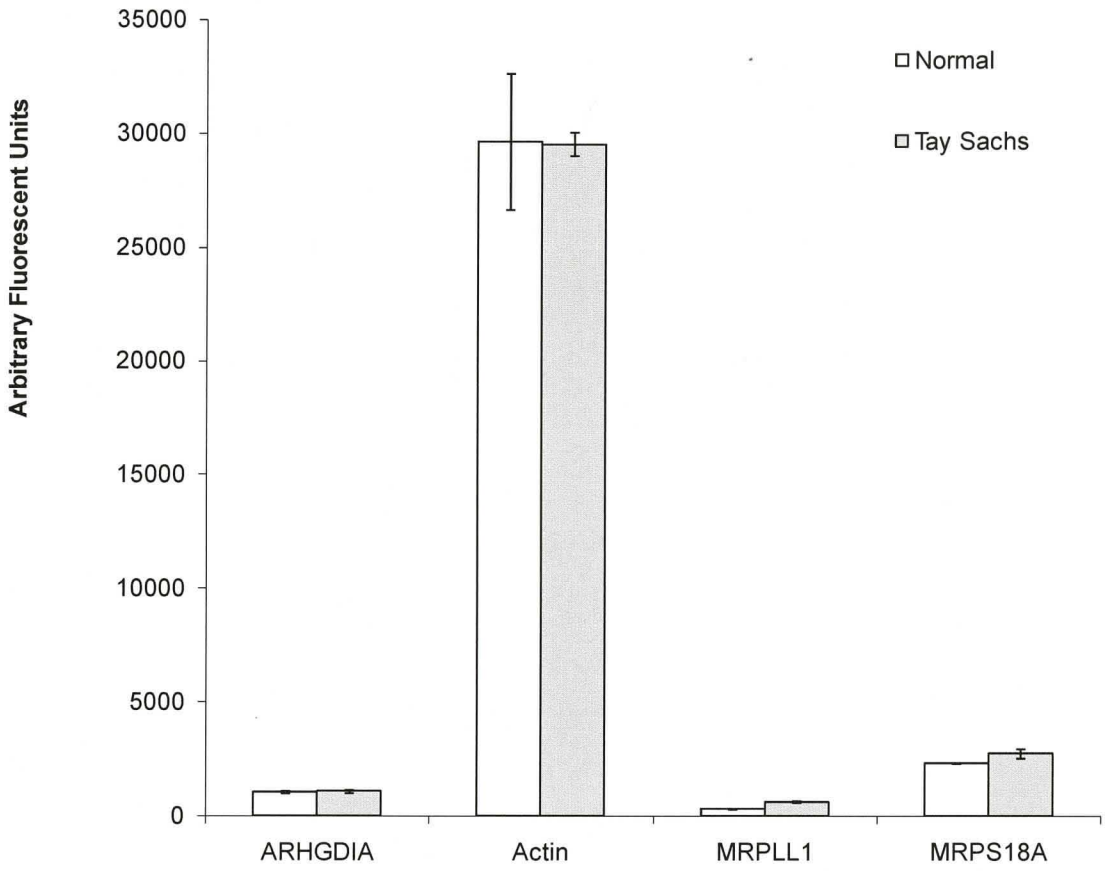

Figure 2: Gene expression levels of housekeeping genes, ARHGDIA, β-actin, MRP11, and MRPS18A show similar expression in both Normal and Tay Sachs cells. Arbitrary Fluorescent Units from SYBR Green Based Real Time PCR analysis was used to assess gene expression levels of four potential control genes. cDNA was generated from 5ug of total RNA extracted from TSD and Normal cells. PCR was performed using primers specific for these control genes. Experiments were performed in triplicate and error bars represent standard error.

.

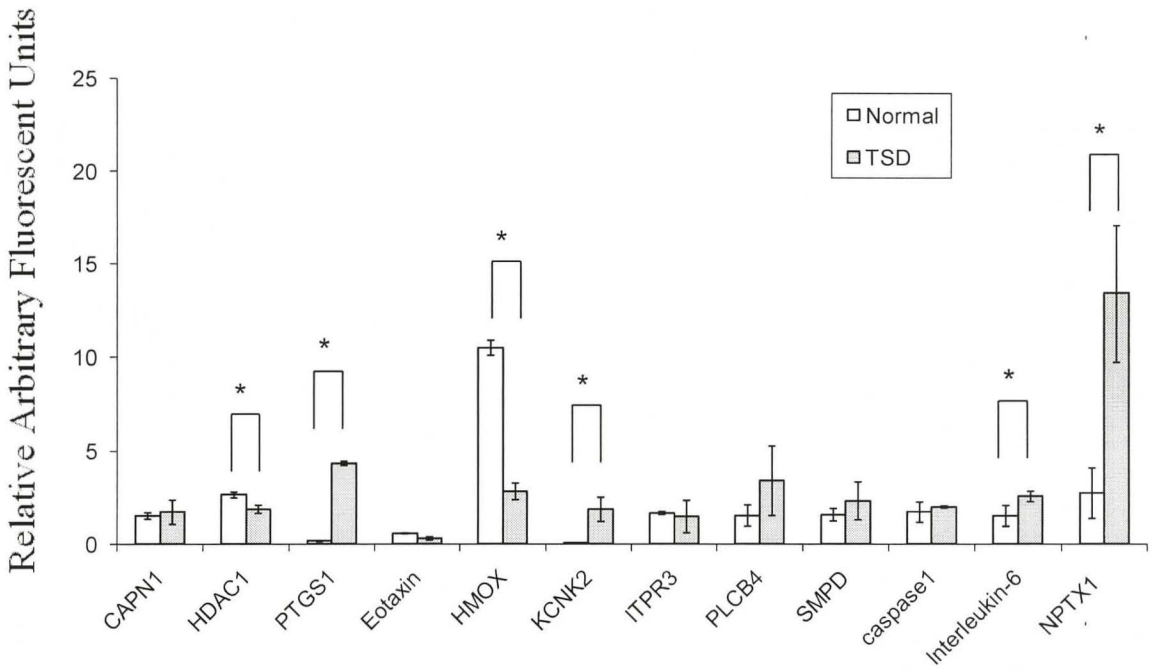

Figure 3: HDAC1, PTGS1, HMOX1, KCNK2, Interleukin 6 and Pentraxin1 gene expression levels are altered in TSD cells when compared to Normal cells. SYBR Green based Real Time PCR was used to compare the expression levels of 12 candidate genes in TSD and Normal neuroglia cells. Six genes were shown to have a difference in gene expression [Columns marked with an asterisk are significantly different, $p<0.05$]. However, gene expression levels of CAPN1, Eotaxin, ITPR3, PLCB4, SMPD and Caspase 1 were similar in TSD and Normal cells. Units are expression level of the gene normalized against that of β-actin. Experiments were performed in triplicate and error bars show standard error.

3.2 Altered gene expression is associated with ganglioside accumulation

To determine if the difference in expression levels seen were indeed related to the accumulation of gangliosides, Tay Sachs cells were incubated with an inhibitor of gangliosides synthesis, NBDNJ. This has previously been shown to reduce ganglioside accumulation, thereby alleviating the disease (Platt et al., 1997). Gene expression was then determined. Our results revealed that NPTX1, HMOX1, KCNK2, and PTGS1 reverted to normal expression in response to NBDNJ (figure 4). To confirm the RNA data, NPTX1 protein levels were examined. Cells were labeled with [^{35}S]methionine and [^{35}S]cysteine and immunoprecipitaiton of NPTX1 was done (Figure 5). This agrees with the RNA data, which shows an increase in Pentraxin in the TSD cells and attenuation with treatment with NBDNJ.

To further correlate the gene expression levels with the disease, another method of alleviating the ganglioside accumulation was used. Previous work has shown that overexpression of sialidase also decreases GM2 accumulation in Tay Sachs cells (Igdoura et al., 1999). Sialidase overexpression results in a 60 percent decrease in pentraxin levels. KCNK2 and PTGS1, however, are unaffected by this treatment (Figure 6).

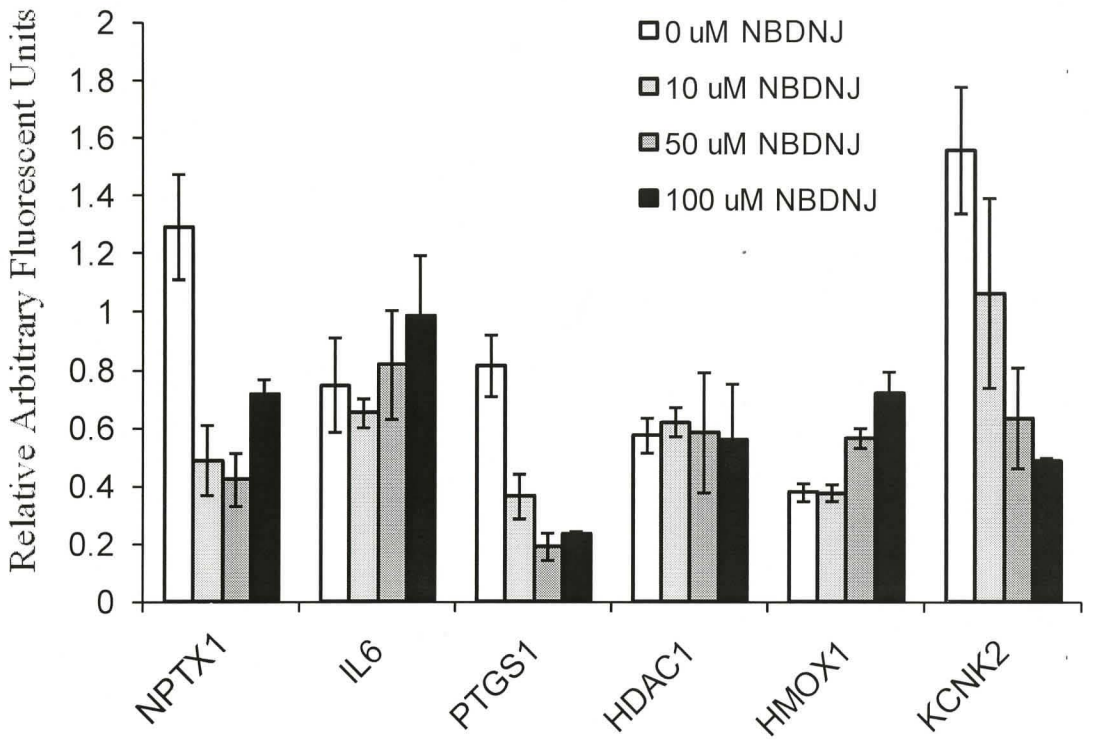

Figure 4: Changes in NPTX1, PTGS1, HMOX1 and KCNK2 gene expression levels in TSD neuroglia are attenuated with NBDNJ treatment. TSD and Normal human neuroglia were treated for 5 days with 0μM, 10μM, 50μM and 100μM of inhibitor N-butyldeoxynojirimycin (NBDNJ). Following incubation, gene expression levels were determined using Real Time PCR and visualized by SYBR Green fluorescence. While Pentraxin, PTGS1, HMOX1 and KCNK2 gene levels were normalized upon treatment, IL6 and HDAC1 gene levels were unresponsive to the inhibitor. PCR was performed using primers specific to these genes. Expression levels of each gene were normalized against those of β-actin and error bars show standard error.

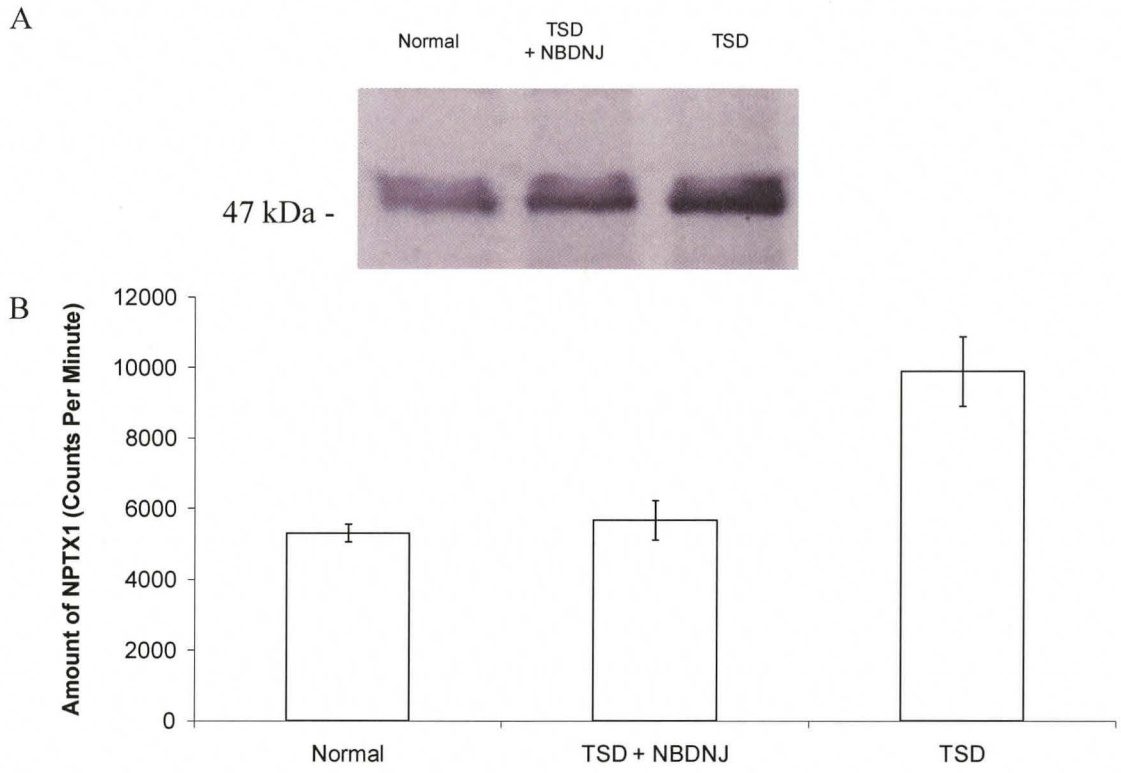

Figure 5: NPTX1 protein is upregulated in Tay Sachs cells and attenuated with treatment of NBDNJ. Cells were treated with 100 μM NBDNJ for 5 days, labeled with [^{35}S]cysteine/methionine and NPTX1 was immunoprecipitated. A) Duplicate samples were run on SDS-PAGE and exposed for 24 hours. B) The bands corresponding to NPTX1 were removed and radioactivity was measured. Bars denote range.

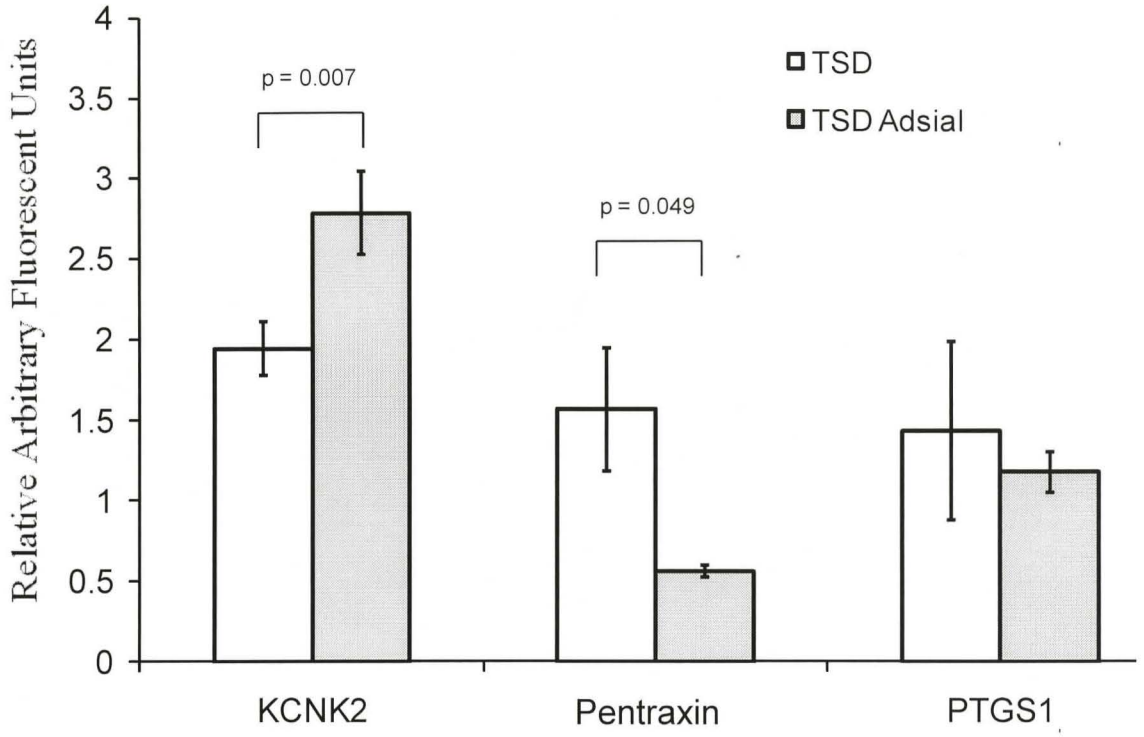

Figure 6: Sialidase overexpression reduces neuronal Pentraxin gene expression levels. TSD neuroglia cells were mock-infected (0 MOI) or infected for 1 hr with AdSial (50 MOI). Following infection, RNA was isolated and NPTX1 mRNA levels were determined using real time quantitative PCR. Gene expression levels were normalized against those of β-actin using SYBR Green based Real Time PCR. The experiment was performed in triplicate and bars indicate standard error.

3.3 Tay Sachs cells are sensitive to AMPA-induced apoptosis

To establish a functional role for the increased NPTX1 expression in Tay Sachs cells, we investigated two pathways in which pentraxin has been involved, potassium deprivation, and glutamate excitotoxicity. In both instances, an increase in pentraxin expression leads to apoptosis (DeGregorio-Rocasolano et al., 2001). We therefore tested the Tay Sachs cells' response to potassium deprivation by culturing them in high potassium media (25mM KCl) and switching to low potassium media (5mM KCl) and then measuring RNA levels of NPTX1. This showed no relationship between potassium levels and pentraxin expression (figure 7).

NPTX1 has been reported to mediate apoptosis in cerebral granular cells via AMPA stimulation and, consequently, glutamate-induced excitotoxicity (Hossain et. al., 2004). Further evidence of the role of excitotoxicity was found when we examined the expression of EAAC1, the glutamate transporter. According to the microarray data, EAAC1 shows a fourfold increase in expression when compared to the normal neuroglia cells. To establish whether this mechanism is present in TSD neuroglia, we tested the effect of AMPA on the expression of NPTX1. In our study, incubation of TSD cells with 300 μM AMPA for 24 hours induces NPTX1 two-fold (figure 8). This is also observed in cells treated with NBDNJ and although there is no statistical significance ($p=0.22$), there is a trend toward a reduction in the extent of pentraxin induction.

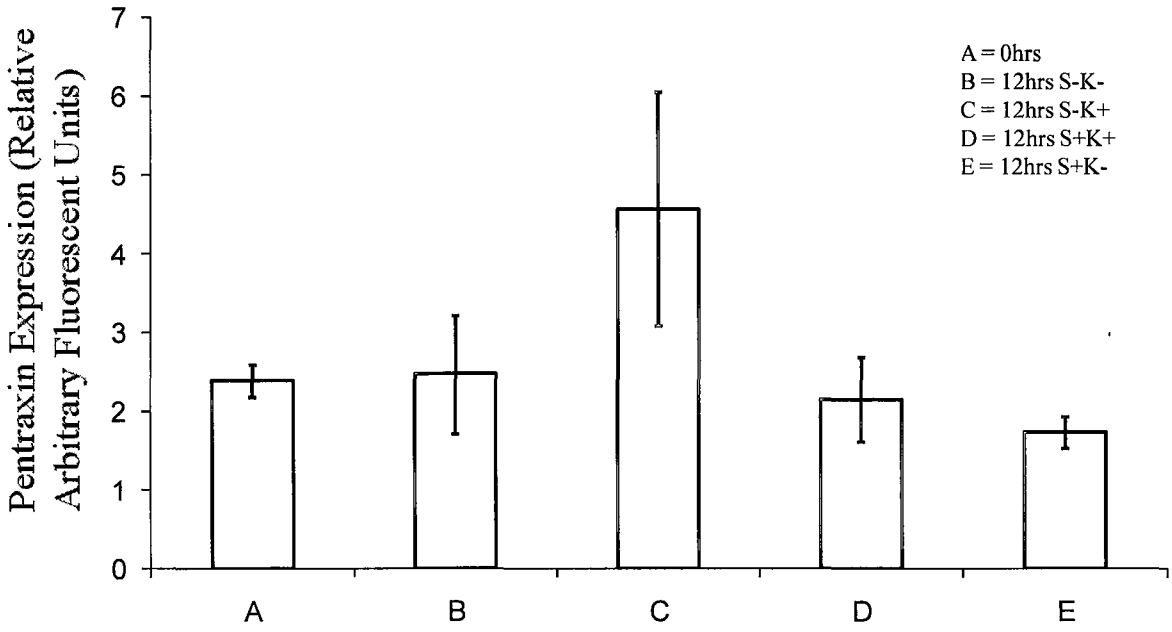

Figure 7: Potassium deprivation does not affect Pentraxin gene expression levels in TSD neuroglia. TSD cells were grown in basal eagles media supplemented for 5 days with 10% FBS and 25mM KCl. Following incubation, cells were treated with serum (S+) or without serum (S-) in the presence of 25mM KCl (K+) or 5mM KCl (K-). Pentraxin mRNA levels were determined by real time quantitative PCR using NPTX1 specific primers. Expression levels were quantified using SYBR green fluorescence units and normalized against those of β-acitn. The experiment was performed in triplicate and error bars denote standard error.

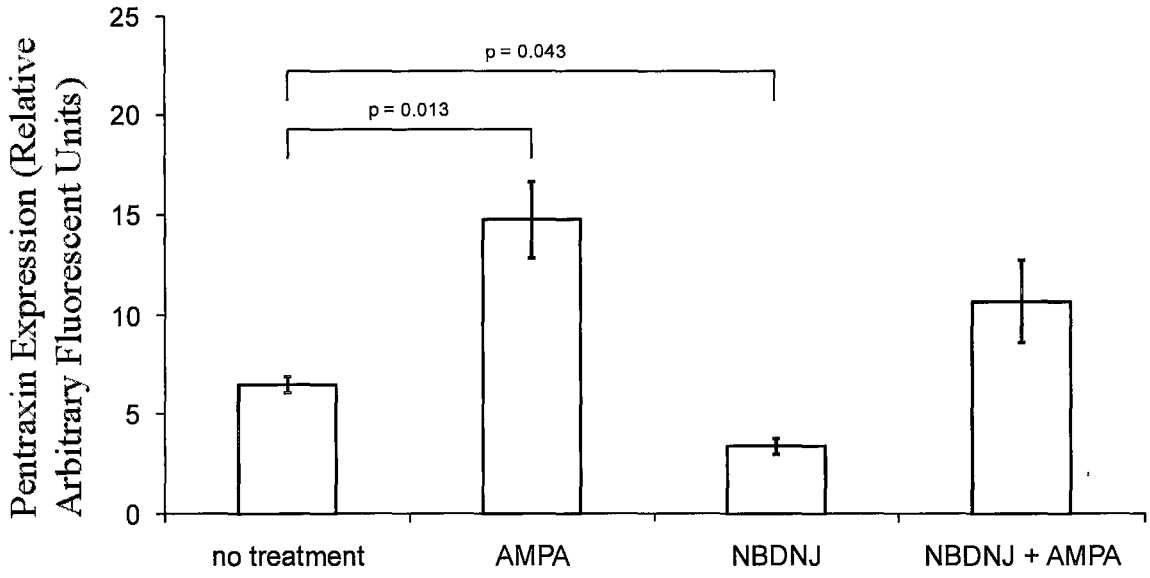

Figure 8: AMPA induced Pentraxin gene expression may not be dependent on ganglioside accumulation only. TSD neuroglia were treated for 5 days with inhibitor NBDNJ. Treatment was followed by the addition of 300μM AMPA for a 24 hour period. Real time quantitative PCR was performed to determine the mRNA levels of Pentraxin. Expression levels were measured using SYBR green fluorescence and normalized against those of β-actin. The experiment was performed in triplicate. Errors bars indicate standard error.

3.4 NBQX reduces attenuates Tay Sachs associated NPTX1 overexpression

To further identify the involvement of NPTX1 and excitotoxicity in the Tay Sachs cells, we examined the effect of the AMPA antagonist, NBQX (2,3-dihydroxy-6-nitro-7-sulfamoyl-benzo[f]quinoxaline-2,3-dione), on NPTX1 expression. Our data indicated that NBQX not only blocks AMPA induced NPTX1 expression but also reduces it by approximately 50 percent, in much the same fashion as NBDNJ (figure 9). This was also observed when we examined protein levels (figure 10).

3.5 NPTX1 colocalizes with EAAC1 and GLUR1

Co-localization of NPTX1 with the AMPA receptor, GLUR1, has been previously shown in cerebral granule cells (DeGregorio-Rocasolano et al, 2001). To investigate the role of NPTX1 in the AMPA sensitivity of the Tay Sachs neuroglia, we examined not only the distribution of NPTX1 and GLUR1, but also that of, the glutamate transporter, EAAC1. Immunocytochemical analysis using antibodies against GLUR1, NPTX1, and EAAC1 show strong NPTX1-GLUR1, as well as NPTX1-EAAC1 colocalization (figure 11). However, this is determined by the density of NPTX1 expression since colocalization with NPTX1 is only observed where pentraxin is expressed in a dense cluster.

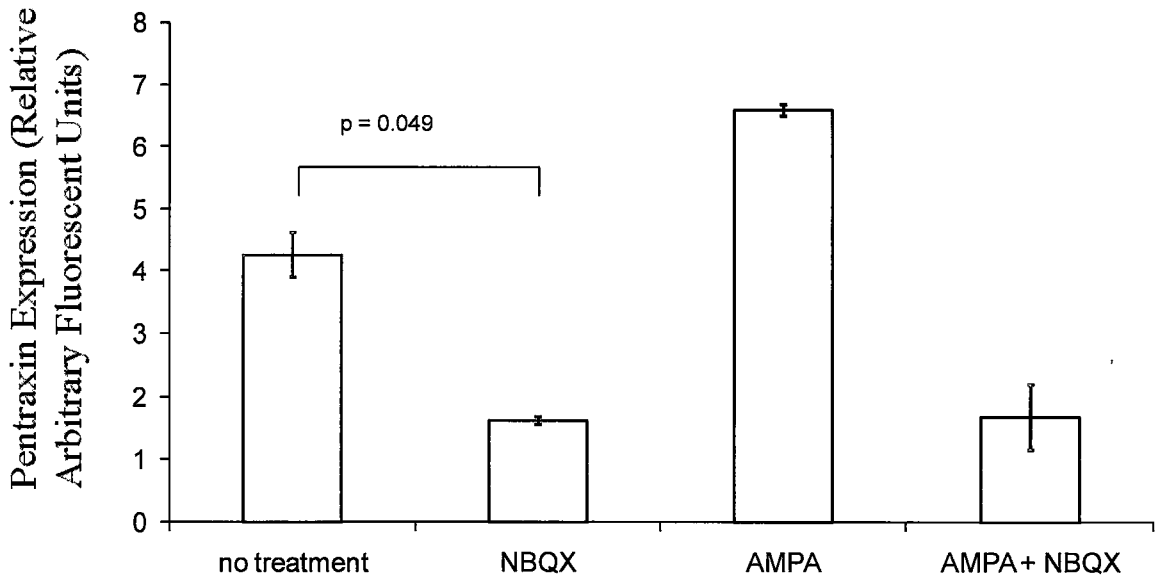

Figure 9: Pentraxin is regulated by glutamate receptor stimulation. TSD cells were treated overnight with 100μM AMPA, 100μM NBQX or 100μM AMPA + 100μM NBQX. Pentraxin gene expression levels were quantitated using real time PCR and measured by SYBR green units. The experiment was performed in triplicate and expression values were normalized against those of β-actin. Errors bars indicate standard error.

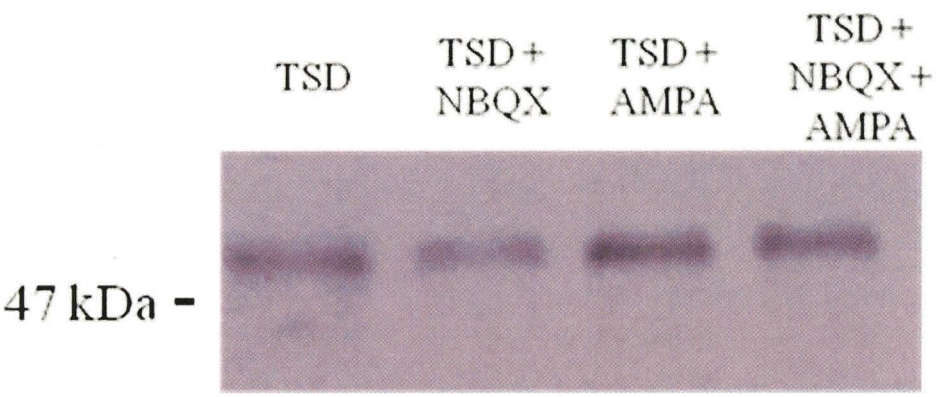

Figure 10: Pentraxin is regulated by glutamate receptor stimulation. TSD cells were treated overnight with 100μM AMPA, 100μM NBQX or 100μM AMPA + 100μM NBQX. TSD cells labeled with [^{35}S]cysteine/methionine were used for immunoprecipiation with NPTX1. Cells treated with NBQX show a reduction in Pentraxin levels. The reduction is blocked however, in the presence of both NBQX and AMPA.

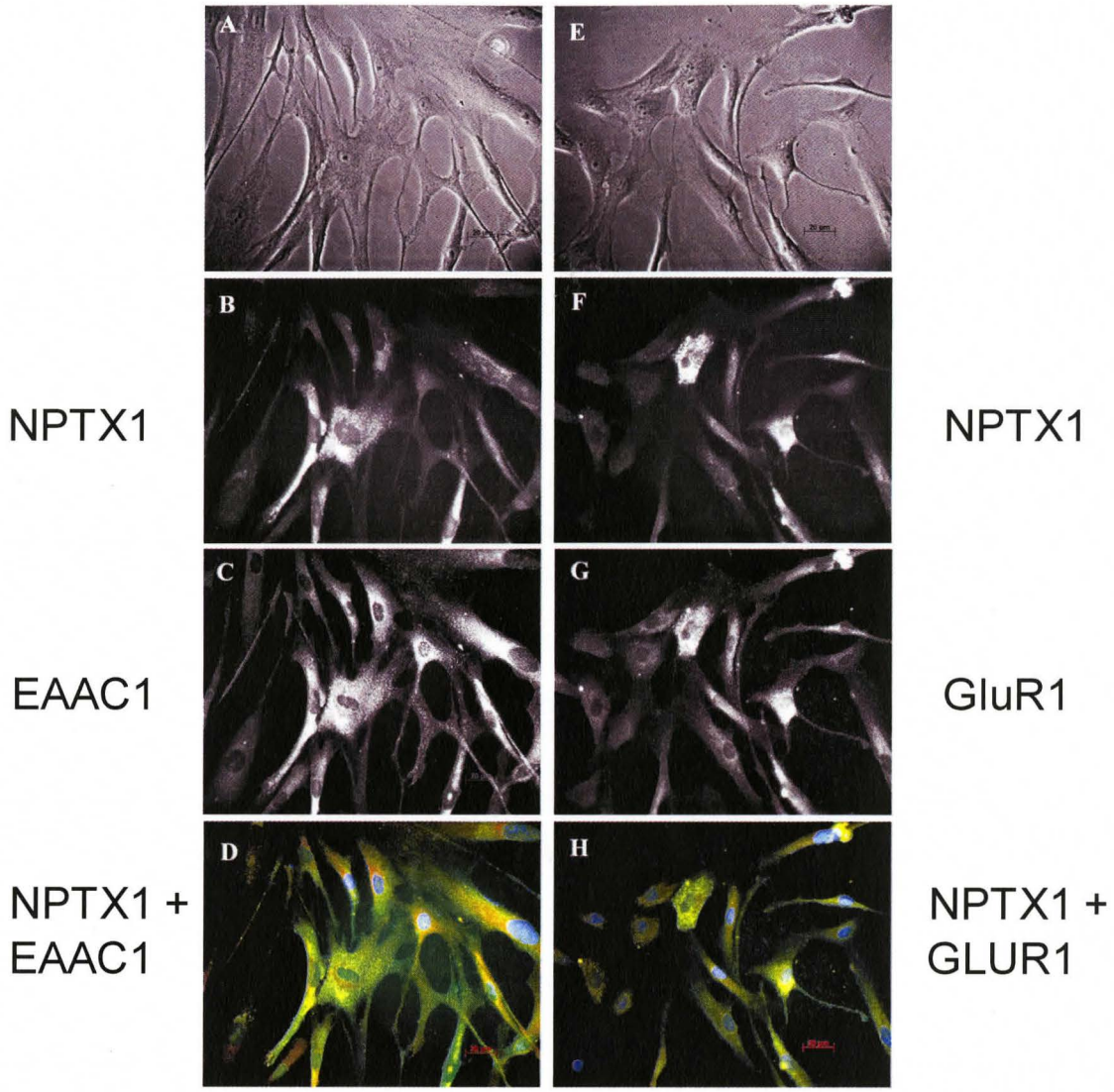

Figure 11: Immunofluorescent co-localization of neuronal pentraxin-1 with either EAAC1 (A-D) or GLUR1 (E-H) in Tay Sachs neuroglia cells. Areas of colocalization are represented by the yellow overlap in panels D and H. Note that colocalization of pentraxin with either EAAC1 or GLUR1 is restricted to FITC of dense NPTX1 staining. A and E were taken under phase contrast, B and F with a FITC filter, and C and G with a texas red filter. Bars indicate 20 μm.

3.6 AMPA induces calcium influx in Tay Sachs cells

Since AMPA receptors consisting of only the GLUR1 subunit are calcium permeable, we measured the calcium influx evoked by glutamate and AMPA in both TSD and normal cells using FURA-2 AM as a detector. As seen is figure 12, neither glutamate nor AMPA evoked any substantial increase in calcium levels. The TSD cells, however, showed rapid increases in calcium levels which were then rapidly rectified.

3.7 Tay Sachs cells are susceptible to AMPA-mediated apoptosis

Since there appears to be an increase in calcium influx upon stimulation of TSD cells with AMPA, then it is probable that there may be an increase in calcium-mediated apoptosis with this treatment. Therefore, we examined the effect of AMPA stimulation on the apoptotic potential of both Tay Sachs and normal neuroglia cells. As seen in figure 13, without AMPA stimulation, both cell types show the same level of apoptosis. With addition of AMPA for 24 hours however, Tay Sachs cells show twice the percentage of apoptotic cells compared to normal neuroglia ($p = 0.007$).

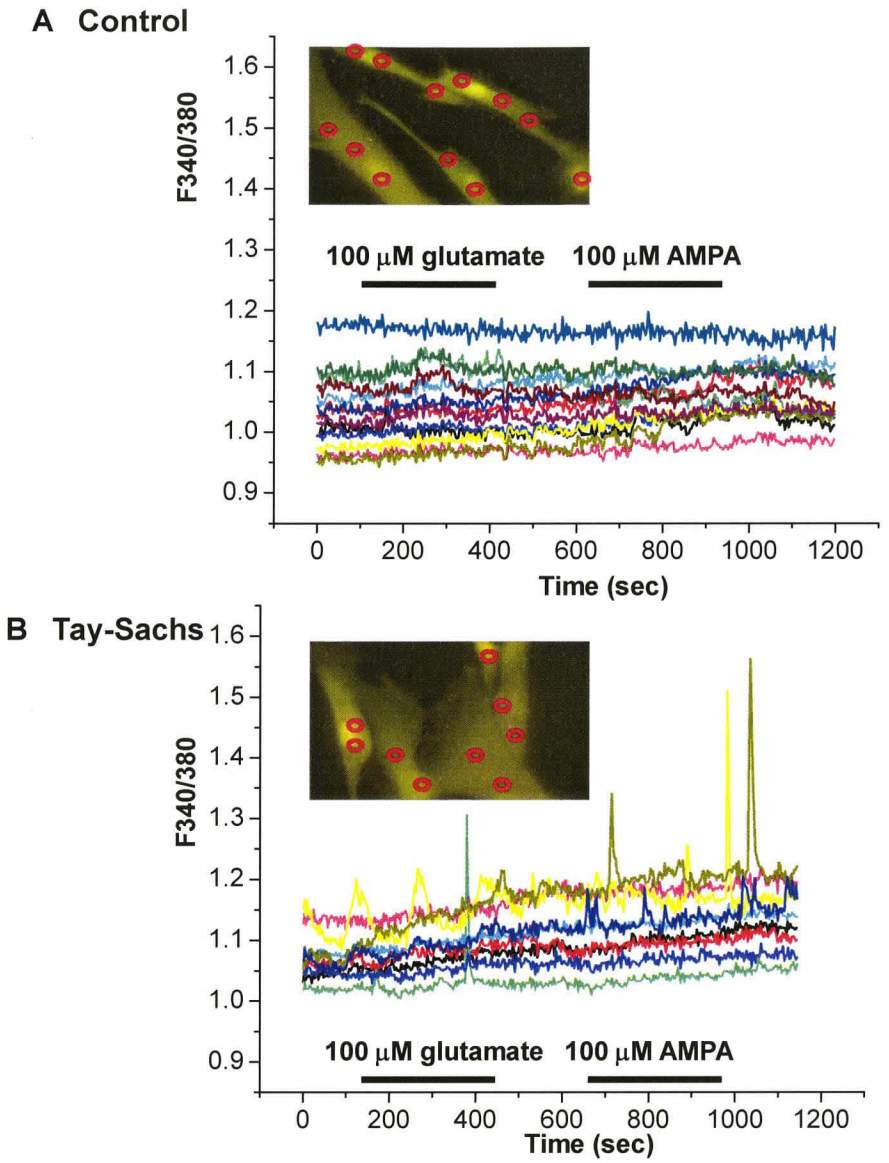

Figure 12: Ratiometric glutamate and AMPA evoked Ca^{2+} signals in normal (A) and Tay-Sachs (B) neuroglia cells. Cells were loaded with 5 mM Fura-2 AM for 20 min at room temperature. Recordings were made at 32-34 °C on cell regions (red circles) which are shown on the images of fura-2 AM loaded -cells. Bath application of glutamate and AMPA for 300 seconds evoked Ca^{2+} transients in Tay-Sachs cells (note Ca^{2+} spikes in some cases), whereas no responses were detected in control cells. Ratiometric Ca^{2+} imaging (F340/380) was performed using a Nikon Eclipse TE2000-U inverted microscope equipped with a Lambda DG-4 high-speed optical wavelength changer, a Hamamatsu OCRCA-ET digital CCD camera, and a Nikon S-Fluor 40x oil immersion objective (NA 1.3). Each trace corresponds to a different cell region.

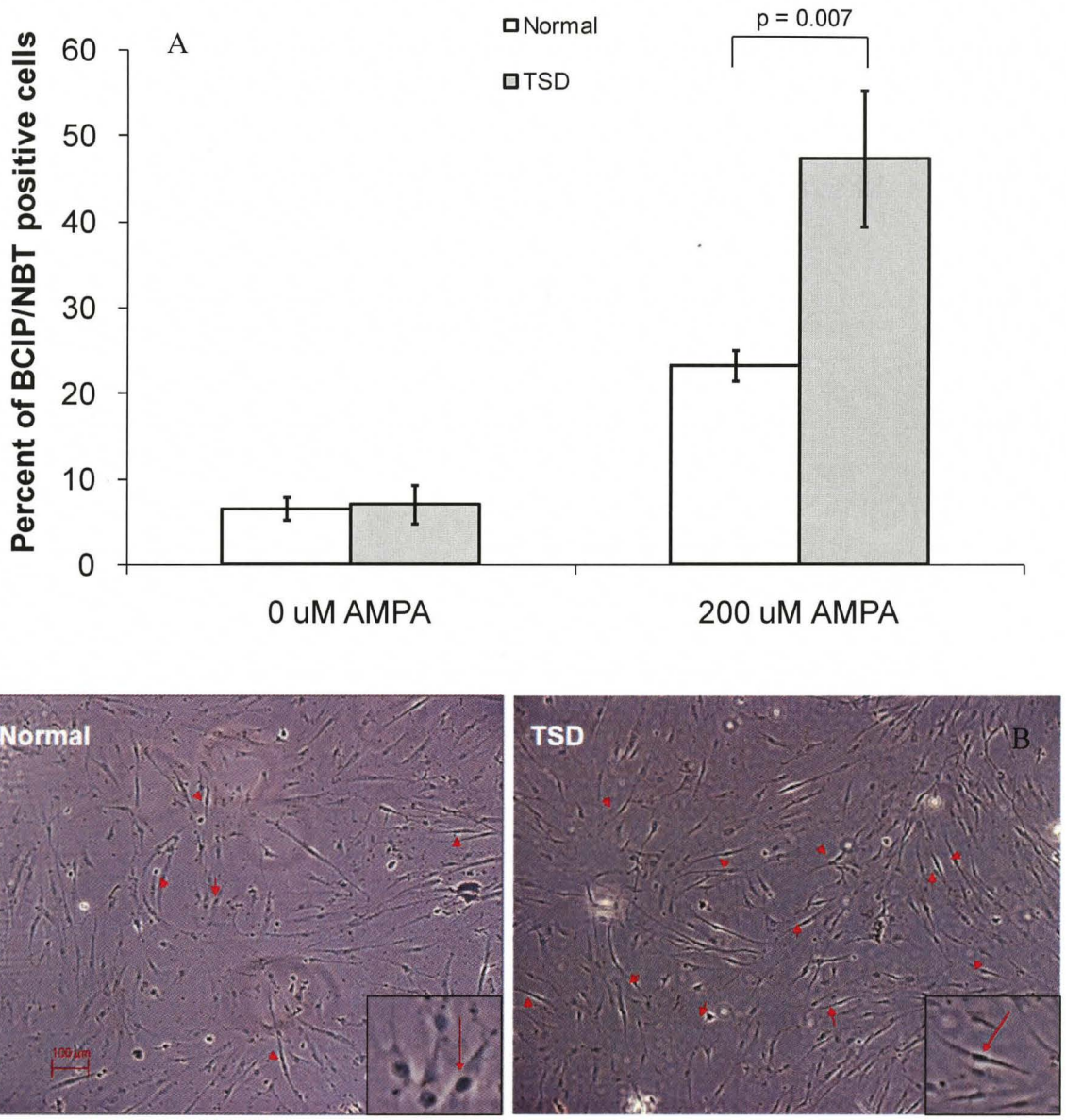

Figure 13: Tay Sachs cells are more susceptible to AMPA-mediated apoptosis. TSD cells were incubated in DMEM supplemented with 10% FBS and treated with 0µM and 200µM AMPA for a 24 hour period. Following treatment, cell death was visualized using an Apoptag kit (Invitrogen) and methyl green counterstaining. (A) The number of cells undergoing apoptosis was scored as a percentage of the total cells. n=3, while error bars denote standard error. (B) Phase contrast images of normal and TSD cells treated with 200 µM AMPA. Apoptotic cells are indicated with red arrows. Scale bar represents 100 µm.

4 Discussion

An effective treatment for Tay Sachs disease has yet to be discovered. Much of the effort has been focused on substrate deprivation. Treatment of ganglioside storage disorders with NBDNJ, a ganglioside inhibitor, has shown promise in reducing ganglioside accumulation and, therefore, in alleviating symptoms in clinical trials of Gaucher patients (Aerts et. al., 2006). Although this seems to be a promising treatment for lysosomal storage disorders, it has its shortcomings since mice treated with NBDNJ have shown a 50 percent decrease in cellular material within their spleen and thymus (Platt et. al., 1997). Therefore, targeting secondary pathways involved in the disease progression may be more beneficial. The mechanistic cascade that causes ganglioside accumulation to result in neurodegeneration is still unclear leaving us with several questions. What pathways are involved in linking ganglioside accumulation and neurodegeneration? What genes are activated or inactivated in response to this accumulation? Answers to these questions will unravel the disease mechanism and potentially enable us to identify new therapeutic targets for the treatment of Tay Sachs disease.

4.1 Tay Sachs Cells Express Abnormal Gene Expression Levels

Our microarray analysis of Tay Sachs and normal neuroglia cells revealed modulation of pathways consistent with the neurodegenerative nature of the disease. These include neuroinflammation pathways including immune response and interleukin signaling as well as metabolic stress pathways such as oxidative and ER stress response. Cluster analysis and PANTHER analysis identified genes involved in glutamate balance and trafficking, which suggests glutamate-mediated excitotoxicity may play a role in the disease. In addition to these findings, our data revealed a number of upregulated genes that have previously been shown to play a role in other neurodegenerative diseases such as Alzheimer's and Huntington's (see Appendix A).

Several groups have examined the possibility of common elements between these diseases. For example, synaptic plasticity and excitotoxicity have been implicated in common neurodegeneration. Studies from Alzheimer's patients indicate that neuronal death alone cannot account for all of the synaptic dysfunction (Buell and Coleman, 1979; Flood and Coleman, 1990; de Ruiter and Uylings, 1987). This is indicative of an interruption of the synaptic signaling pathway and has been confirmed in a transgenic model of Alzheimer's (Stern et al. 2004). Amyloid-β has also been shown to be toxic due to elevation of postsynaptic calcium influx and NMDA internalization (Small et. al., 2001; Snyder et. al., 2005). Several genetic markers have been identified in Huntington's disease which are implicated in plasticity and excitotoxicity. In a clinical study of two hundred ninety-three Huntington's patients, genotypic variation of the glutamate receptor, GluR6 (Rubinsztein et al. 1997), was identified in those patients with symptoms

more severe than was predicted based on the extent of CAG repeats in the IT15 gene. In a similar fashion, the NMDA receptor subunits NR2A and NR2B have been identified as markers in Huntington's disease families (Arning et al. 2005). This is supported by the disrupted NMDA receptor function seen in other Huntington's disease models. However, there is extensive evidence for disrupted NMDA receptor function in Huntington's disease models (Hansson et al. 1999; Levine et al. 1999; Sun et al. 2001 Luthi-Carter et al. 2003). In addition, in a mouse model of Huntington's, ligand binding to several kainate and AMPA receptors in the postsynaptic neuron was impaired as well (Cha et al. 1998). This offers evidence that while many of the neurodegenerative diseases (common or rare) result from different genetic mechanisms, the pathophysiology behind these diseases may share some common features.

To isolate genes that function more specifically in Tay Sachs disease, we focused on factors that were involved in pathways correlated with a ganglioside storage disorder. First, we examined the involvement of sphingomyelin phosphodiesterase-1 (SMPD), a protein involved in glycosphingolipid regulation and metabolism that coverts sphingomyelin into ceramide, a pro-apototic lipid and the backbone for all gangliosides (Pettus et. al., 2002). Downregulation of this gene in TSD cells could possibly be a pro-survival mechanism.

Second, since inflammation is a major hallmark of lysosomal storage disorders, we investigated the upregulation of interleukin 6 (IL6) and the IL1β activating enzyme, caspase 1. As both genes have been shown to be involved in neuroinflammatory disease

(Basu et. al., 2004), we propose a role for IL6 and caspase I in a proinflammatory response in TSD. The IL6 pathway is controlled by signal transducer and activator of transcription (STAT) proteins, STAT1 and STAT3, which are regulated by histone deacetlyase 1 (HDAC1) (Klampfer et. al., 2004). HDAC1 expression levels were also upregulated in our array. Our data also identified Eotaxin, a chemokine which exacerbates inflammation by recruiting eosinophils (Menzies-Gow et. al., 2002), prostaglandin synthase 1 (PTGS1), also known as cyclooxygenase 1 (COX1), an inflammatory marker that aids in the synthesis of arachidonic acid derived hormones (Wallace, 1999), and heme oxygenase 1 (HMOX1), a gene involved in neurodegeneration. Inhibition of HMOX1 results in increased oxidative neurotoxicity in Alzheimer's disease (Orozco-Ibarra et. al., 2006).

Third, we observed that the expressions of several calcium-dependant genes were altered in Tay Sachs cells. Calcium balance is an important cellular process that is highly sensitive to ER stress, a response that may be induced in Tay Sachs cells. Phospholipase C (PLCB4) synthesizes Inositol triphosphate which binds to the ER receptor ITPR3 and triggers release of endoplasmic stores of calcium and consequently, ER stress. Our data show that both PLCB4 expression is increased, while ITPR3 expression is decreased in Tay Sachs cells. Additional evidence of disrupted Ca^{2+} homeostasis is seen with the downregulation of Calpain, a calcium dependant protease.

Fourth, gangliosides have been shown to alter activity of potassium channels (Chen et. al., 2005). Since potassium homeostasis is so important in maintenance of

membrane potential and proper neuron function, they may be involved in the Tay Sachs disease mechanism. KCNK2, an outwardly rectifying potassium channel, was found to be upregulated in Tay Sachs neuroglia.

Finally, glutamate excitotoxicity is a major mechanism of neuronal apoptosis that relies heavily on ion imbalance. Overstimulation of glutamate receptors leads to an increase in intracellular potassium and calcium. This increase of cation concentrations not only disrupts the membrane potential but also induces an apoptotic cascade. It has been linked to other neurodegenerative diseases such as cerebral ischemia (Lo et. al., 1997). All the previously mentioned calcium homeostasis proteins, PLCB4, ITPR3, and calpain are also involved in events downstream of excitotoxicity. Most significantly, we found an upregulation of neuronal pentraxin 1 (NPTX1), a gene that is directly involved in excitotoxicity, since it clusters glutamate receptors to the synapse. Increased aggregation of these receptors to the synapse increases sensitivity of cells to glutamate-induced depolarization (O'Brien et. al., 1998). Knockdown of pentraxin prevents glutamate receptor mediated cell death and is therefore protective against excitotoxicity (Hossain et. al., 2004). NPTX1 is not the only neuronal pentraxin implicated in proper neuron function. Neuronal pentraxin 2 (NPTX2) is induced upon neuron stimulation, persists for an hour and returns to basal levels, and also promotes neurite outgrowth (Tsui et. al., 1996).

4.2 Pentraxin is Upregulated in Tay Sachs Cells

Using NBDNJ to alleviate ganglioside accumulation in the diseased cells, we observed expression levels of several genes to be comparable with those of the normal cells, and therefore associated those genes with the disease. We discovered that NPTX1, PTGS1, HMOX1 and KCNK2 gene expression levels reverted to normal levels when exposed to NBDNJ, implicating them as molecular factors associated with TSD disease.

Sialidase, an enzyme responsible for cleaving sialic acid from sugar moieties on proteins and glycolipds, has also been shown to reduce ganglioside accumulation (Igdoura et al., 1999). We expect that sialidase upregulation should have the same effect as NBDNJ administration. Only NPTX1 expression levels revert to normal levels upon sialidase exposure. KCNK2 and PTGS1 however, are not eliminated as possible markers for the disease since this may simply be due to secondary effects of the sialidase treatment. Collectively, our findings implicate NPTX1 as a marker for Tay Sachs Disease.

4.3 Ganglioside Accumulation in Tay Sachs Cells and Increased Pentraxin Levels

Examining the function of pentraxin may help us understand the physiological effect related to the disease. Pentraxins are a group of proteins further divided into the short pentraxins, C-reactive protein (CRP) and serum amyloid protein (SAP) and the long pentraxins, neuronal pentraxin 1 and 2, and neuronal pentraxin receptor. The short

pentraxins are expressed highly in the liver and have been thoroughly characterized as inflammatory markers. SAP has even been characterized as calcium dependant lectin, and can bind to sugar moieties (Emsley et. al., 1994). This ability to interact with carbohydrate chains is also observed in long pentraxins and is believed to be of vital for proper function (Tsui et. al., 1996). The involvement of pentraxin during apoptosis has been shown via two distinct pathways, potassium deprivation and glutamate receptor stimulation. Our potassium deprivation study shows no changes in pentraxin levels in response to potassium deprivation. One explanation is that pentraxin is not responsive to potassium homeostasis in our cells, since, unlike neurons and cerebral granule cells, neuroglia do not require potassium-enriched media. Another possibility is that this is an abnormal phenotype and that the prevention of pentraxin induction by potassium deprivation is a result of Tay Sachs disease. Further study would be needed to investigate these possibilities.

Pentraxin has been shown to localize with GLUR1 (Hossain et. al., 2004). GLUR1 receptor functions by importing sodium and calcium into the cell in response to glutamate stimulation. Our study not only confirms this NPTX1-GLUR1 association but also shows colocalization of pentraxin and the glutamate transporter, EAAC1. This adds further evidence that pentraxin is modulating excitotoxicity as the glutamate transporter is responsible for uptake of glutamate to decrease its effect. It is the balance between the activity of the receptors and the transporters that dictate the effect of glutamate on the neuron. The colocalization implies that pentraxin may be acting at the site of glutamate stimulation.

To elucidate the role of pentraxin in Tay Sachs disease we focused our attention on the interaction of pentraxin with these receptors. The ability of glutamate to bind multiple receptors such as NMDA and kainite receptors allows us to use AMPA, a glutamate agonist, to specifically target GLUR1-4 receptors. AMPA causes a two-fold increase in pentraxin expression. NBDNJ appears to, although not significantly, reduce this pentraxin induction. As previously stated, stimulation of GLUR1 by AMPA increases pentraxin expression in a dose-dependent manner. This results in an increased clustering of AMPA receptors to the synapse and in turn, this increases a cell's sensitivity to glutamate stimulation (King et. al., 2006). The colocalization of NPTX1 with GLUR1 and EAAC1 support this influence of pentraxin on glutamate sensitivity. The increased pentraxin expression in the Tay Sachs cells may therefore be a result of constitutively active glutamate receptors by gangliosides. This is supported by reduction of the endogenous pentraxin expression to that of normal cells by not only NBDNJ, but also NBQX.

The mechanism of pentraxin upregulation in response to endogenous ganglioside accumulation is still unclear. However, since the long pentraxins are expressed in response to a change in membrane potential, it is possible that ganglioside accumulation disrupts ionic homeostasis in the cell by modulating ion channels, a well characterized event (Carlson et. al., 1994; Rahmann et. al., 1992; Chen et. al., 2005; Takigawa and Yasuda, 1995). Gangliosides also modulate several other receptor-mediated signaling pathways. GM1 binds tightly with TrkB, the nerve growth factor receptor and enhances the autophosphorylation of the receptor three-fold (Mutoh et. al., 1995). GM3 is an

inhibitor of tyrosine kinase involved in platelet derived growth factor signaling (Bremer et. al., 1984). GM3 also associates with fibroblast growth factor receptor and inhibits its autophosphorylation thereby reducing Mitogen-Activated Protein Kinase (MAPK) activity (Toledo et. al., 2005). Based on this evidence, it is probable that the ganglioside accumulation is effecting receptor function to induce pathways involved in Tay Sachs disease.

4.4 Lipid rafts, gangliosides, and excitotoxicity

Gangliosides and other glycosphingolipids regulate membrane fluidity and structure of lipid rafts. As major components of rafts, ganglioside can regulate and effect intracellular signaling from these structures. For example, upon cellular swelling, calcium activated potassium channels, such as KCNN4, are activated to rebalance osmolarity (Barfod et. al., 2007). During this process, plasma membrane localization of KCNN4 not only increases, but so does its association with lipid rafts. Even more interesting is the time dependant increase of KCNN4-GM1 colocalization during this process, implicating gangliosides as a mediator of the clustering of these ion channels into lipid rafts. A similar relationship between localization of gangliosides with voltage gated sodium ion channels in rabbits treated with anti-GM1 antibody (Susuki et. al., 2007). Treated animals suffered severe neuromuscular dysfunction as a result of a reduction in the clustering of voltage gated sodium channels in the neurons. Once again, the clustering of receptors by gangliosides provides an important physiological function.

This provides a logical location for a ganglioside accumulation to affect glutamate-induced signaling pathways but would require the localization of AMPA receptors to lipid rafts as well. In a study of the composition of the dendritic raft of neurons in the rat forebrain, this occurrence was established (Suzuki et. al., 2001). Isolation of the dendritic raft from the post-synaptic region show enriched GLUR1-GlUR4 immunoreactivity. Also present in this region were several other signaling molecules including CaMKII, TrkB, EGFR, and Erk2. As previously stated, GM1 regulates the phosphorylation and therefore activity of Trk, a component of this dentritic raft (Mutoh et. al., 1995). This receptor is also involved in modulation and clustering of glutamate receptors at the synapse thereby providing further association between ganglioside function and excitotoxicity (Elmariah et. al., 2004). It has also been shown that even nanomolar concentrations of GM2 and GT1b activate PKA and CaMKII (Higashi and Chen, 2004). The direct binding between the extracellular domain of EGFR and GM3 was shown to be the mechanism for the inhibitory effect of the ganglioside on the receptor while another study shows that GD1a has a stimulatory effect on this receptor (Miljan et. al., 2002; Li et. al., 2001). Therefore, it is plausible that gangliosides may also affect other components, such as the glutamate receptors in this signaling-rich domain is plausible. Previous research has shown that AMPA-receptor internalization of AMPA receptors is enhanced in raft depleted neurons (Hering et. al., 2003). It is, therefore, clear that lipid rafts aid in the stabilization of AMPA receptors at the membrane, a process that may in fact be due to the ganglioside content of the membrane. This is further evidence implicating ganglioside accumulation with excitotoxicicty.

4.5 Calcium and lysosomal storage disorders

Imbalances in calcium homeostasis have been previously implicated in lysosomal storage disorders. In a previous study, rat hippocampal neurons cultured with conduritol b-epoxide (CBE) and glutamate excitotoxicity was examined (Pelled et. al., 2000). CBE is an inhibitor of glucocerebrosidase, the enzyme deficient in Gaucher patients. After 3 hours in the presence of 10 mM glutamate, the CBE treated and untreated cells showed 55% and 25% apoptosis respectively. By inhibiting release of reticular calcium stores, this apoptosis was reduced to that of the CBE-untreated cells thereby implicating the ER-stress pathway. Further study of GM2 gangliosidosis from this group revealed increased ER calcium release and decreased reuptake via the SERCA (Pelled et al, 2003). Further support for this comes from the discovery of a direct relationship between levels of glucosylceramide and release of reticular calcium via the ryanodine receptor in cells from a Gaucher patient (Lloyd-Evans et al, 2003). However, these observations may be intermediate response. The ganglioside accumulation may be inducing calcium influx via the glutamate receptors which then activates then enhances ER calcium release and the ER stress response. This is substantiated by studies illustrating that inhibition of the ER stress pathway eliminates apoptosis from overstimulation of glutamate receptors (Sokka et. al., 2007). Concurrent with our data using Tay Sachs cells, the upregulation of NPTX1 has been observed in a Gaucher patient's cerebellum cells (Myerowitz et. al., 2004). The occurrence of the increased pentraxin from this study along with the excitotoxicity results from Pelled et. al. suggest that this is a common mechanism that may account for the

apparent involvement of the ER-stress response seen in lysosomal storage disorders and may even be implicated in other neurodegenerative diseases.

4.6 Proposed disease model: gangliosides, excitotoxicity, and protein kinase C

In several studies, gangliosides and protein kinase C activity have been correlated. Using radioactive ganglioside, association of GM2 with several proteins, including PKC, at the membrane has been established (Sonnino et. al, 1992). Treatment of cells with GT1b has been found to increase phosphorylation of annexin II, a PKC substrate (Katoh and Miyamoto, 1996). PKC activation decreases the concentration of gangliosides exposed to the extracellular space without decreasing total membrane gangliosides (Palestitni et al, 1998). Glial activation by gangliosides also results in activation of PKC (Min et al, 2004). This modulation of PKC activity by gangliosides may therefore be involved in the neurodegeneration observed in Tay Sachs patients.

Furthermore, changes in PKC activity can drastically effect glutamate excitotoxicity due to its effect on the GLUR1. PKC phosphorylates GLUR1 at serine-818, a requirement for long term potentiation. This study also illustrates that the phosphorylation increases the current of calcium into the cell (Boehm et. al., 2006). More importantly, treatment of cerebral granule cells with glutamate causes an induction of PKC and translocation of the protein from the cytosol to the membrane. Although their report offers evidence that GM1 inhibits this translocation (Vaccarino et al, 1997), other groups have reported the converse and show a marked increase in PKC translocation

from the cytosol to the membrane in response to gangliosides (Yada et al, 1991; Garafallo et al, 2002). These results illustrate the ability of gangliosides to activate PKC-mediated phosphorylation of membrane proteins. This implicates the involvement of gangliosides in regulation of the phosphorylation of PKC substrates, including GLUR1. Evidence exists to support that addition of glutamate to cerebral granule cells not only activates PKC, but also disrupts PKC-ganglioside interactions (Masserini et. al., 1998). Gangliosides have also been shown to activate Ca2+/calmodulin-dependent protein kinase II (CaM KII), another kinase shown to phosphorylate GLUR1 and aid excitotoxicity (Higashi and Chen, 2004).

From this, we can establish a possible model for Tay Sachs disease. Ganglioside accumulation may cause enhanced phosphorylation and increase activity of GLUR1 mediated by either PKC or CaM KII. This may then be the stimulus responsible for the increased expression of pentraxin, thereby increasing glutamate receptor clustering. This mechanism, therefore, accounts for the hypersensitivity to AMPA induced apoptosis seen in Tay Sachs cells. The reduction of NPTX1 in the presence of NBDNJ is due to the alleviation of the ganglioside accumulation, whereas the reduction of NPTX1 by NBQX treatment is a result of inactivating the glutamate receptor.

4.7 Future directions

There are several key components to the relationship between ganglioside accumulation and excitotoxicity. Based on our model, inhibition of neuronal pentraxin should reduce adverse symptoms associated with a ganglioside storage disorder. Therefore, treatment of Tay Sachs cells with RNAi against neuronal pentraxin should result in decreased excitotoxicity and decreased calcium influx in response to AMPA. Further evidence for excitotoxicity in LSD's would be ascertained by treatment of the Sandhoff mouse model with NBQX, the GLUR1 antagonist. This should theoretically improve the lifespan of the animal, which normally dies within 4 months of age. Finally, with the pentraxin knockout mouse available, crossing this with the *hexb* knockout mouse would determine the effect of pentraxin in this ganglioside storage disorder.

4.8 Conclusion

Our studies have shown that pentraxin expression levels are upregulated in Tay Sachs cells and that this increase is functionally linked to ganglioside. Our ability to regulate pentraxin levels using the AMPA antagonist NBQX suggests that NBQX may be utilized as a possible therapy for Tay Sachs disease. The experimental evidence strongly implies that excitotoxicity may be one of the earlier signaling pathways in the disease progression. Inducing excitotoxicity mechanisms may account for the presence of several calcium dependant genes, such as those investigated in this study. Glutamate channels allow for the influx of calcium and activation of calcium dependant proteins such as the Sarco/Endoplasmic Reticulum Ca^{2+}-ATPase. More importantly these channels are

necessary for proper functioning of pathways such as ER stress, which has been shown previously to play a role in ganglioside accumulation diseases (d'Azzo et. al., 2006). Further study into the regulation of pentraxin by NBQX in the Sandhoff mouse would elucidate whether this is the case. NBQX has been proven to be a neuroprotector in several neuroinflammatory diseases such as cerebral ischemia (Lo et. al., 1997), spinal cord contusion (Rosenberg et. al., 1999), and multiple sclerosis (Kanwar, 2005) adding weight to its benefit as a treatment for Tay Sachs disease. Finally, our findings indicate that pentraxin upregulation is a result of ganglioside accumulation, and may therefore be a possible therapeutic target for the treatment of Tay Sachs disease.

References

Aerts JM, C.E. Hollak, R.G. Boot, J.E. Groener, M. 2006. Maas Substrate reduction therapy of glycosphingolipid storage disorders. *J Inherit Metab Dis* **29(2-3)**:449-56.

Arning L., P.H. Kraus, S. Valentin, C. Saft, J. Andrich, J.T. Epplen, 2005. NR2A and NR2B receptor gene variations modify age at onset in Huntington disease. *Neurogenetics* **6:** 25–28.

Basu A, J. K. Krady, S. W. Levison. 2004. Interleukin-1: A Master Regulator of Neuroinflammation. *Journal of Neuroscience Research* **78:**151–156

Bardfod, E. T., A.L. Moore, M.W. Roe, S.D. Lidofsky, 2007. Ca^{2+}-activated IK1 Channels Associate with Lipid Rafts upon Cell Swelling and Mediate Volume Recovery *J. Biol. Chem.* **282:** 8984–8993

Benjamin A.M. and J.H. Quastel, 1975. Metabolism of amino acids and ammonia in rat brain cortex slices in vitro: a possible role of ammonia in brain function. *J. Neurochem.* **43:** 1369–1374.

Boehm J, M.G. Kang, R.C. Johnson, J. Esteban, R.L. Huganir, R. Malinow, 2006. Synaptic incorporation of AMPA receptors during LTP is controlled by a PKC phosphorylation site on GluR1. *Neuron* **(2):**213-225

Boulter J, M. Hollmann, A. O'Shea-Greenfield, M Hartley, E. Deneris, C. Maron, S Heinemann. 1990. Molecular cloning and functional expression of glutamate receptor subunit genes. *Science* **31:** 249(4972):1033-7.

Bremer E.G., S. Hakomori, D.F. Bowen-Pope, E. Raines, R. Ross, 1984. Ganglioside-mediated modulation of cell growth, growth factor binding, and receptor phosphorylation. *J Biol Chem* **259(11):** 6818-6825

Buell S. J. and P.D. Coleman, 1979. Dendritic growth in the aged human brain and failure of growth in senile dementia. *Science* **206**: 854–856.

Carafoli, E., 1987, Intracellular Calcium Homeostasis. *Ann. Rev. Biochem.* **56**: 395-433

Carlson R.O., D. Masco, G. Brooker, S. Spiegel, 1994. Endogenous ganglioside GM1 modulates L-type calcium channel activity in N18 neuroblastoma cells. *J Neurosci* **14(4):**2272-2281

Cha JH, C.M.Kosinski, J.A.Kerner, S.A.Alsdorf , L.Mangiarini, S.W.Davies , J.B.Penney, G.P.Bates , A.B. Young. 1998. Altered brain neurotransmitter receptors in

transgenic mice expressing a portion of an abnormal human huntington disease gene. *Proc Natl Acad Sci U S A.* **95**(11):6480-5

Chen, X., S. Chi, M. Liu, W. Yang, T. Wei, Z. Qi, F. Yang, 2005. Inhibitory effect of ganglioside GD1b on K+ current in hippocampal neurons and its involvement in cell apoptosis suppression. *Journal of Lipid Research* **46:** 2580-2585

Colbourne F, S.Y. Grooms, R.S. Zukin, A.M. Buchan M.V.Bennett 2003. Hypothermia rescues hippocampal CA1 neurons and attenuates down-regulation of the AMPA receptor GluR2 subunit after forebrain ischemia. *Proc Natl Acad Sci U S A.* **100**(5):2906-10. Epub 2003 Feb 26.

Cox,T., R.Lachmann, C.Hollak, J.Aerts, W.S.van, M.Hrebicek, F.Platt, T.Butters, R.Dwek, C.Moyses, I.Gow, D.Elstein, A.Zimran. 2000. Novel oral treatment of Gaucher's disease with N-butyldeoxynojirimycin (OGT 918) to decrease substrate biosynthesis. *Lancet* **355**: 1481-1485.

Danbolt N. C., 2001. Glutamate uptake. *Prog. Neurobiol.* **65:** 1–105.

d'Azzo,A., A.Hoogeveen, A.J.Reuser, D.Robinson, H.Galjaard. 1982. Molecular defect in combined ß-galactosidase and neuraminidase deficiency in man. *Proc Natl Acad Sci U S A* **79(15):** pp. 4535-4539.

d'Azzo A, A. Tessitore, R. Sano. 2006. Gangliosides as apoptotic signals in ER stress response. *Cell Death Differ.* **13(3)** pp.404-414.

DeGregorio-Rocasolano,N., Gasull,T., Trullas,R., 2001. **O**verexpression of neuronal pentraxin 1 is involved n neuronal death by low K+ cerebellar granule cells. *J. Biol. Chem* **276**: 796-803

Diamond P., A. McGinty, D. Sugrue, H.R. Brady, C. Godson, 1999, Regulation of leukocyte trafficking by lipoxins. Clin. Chem. Lab Med. **37**, 293–297.

Dickey CA, J.F.Loring, J.Montgomery, M.N.Gordon, P.S.Eastman , D.Morgan 2003 Selectively reduced expression of synaptic plasticity-related genes in amyloid precursor protein + presenilin-1 transgenic mice. *J Neurosci.* **23**(12):5219-26.

Draghici,S., P.Khatri, P.Bhavsar, A.Shah, S.A.Krawetz, M.A.Tainsky. 2003. Onto-Tools, the toolkit of the modern biologist: Onto-Express, Onto-Compare, Onto-Design and Onto-Translate. *Nucleic Acids Res.* **31**: 3775-3781.

Drew P. D., P.D. Storer, J.H. Xu, J.A. Chavis, 2005, Hormone regulation of microglial cell activation: relevance to multiple sclerosis. Brain Res. Rev. **48**, 322–327.

Eikelenboom,P., J.M.Rozemuller, G.Kraal, F.C.Stam, P.A.McBride, M.E.Bruce, H.Fraser. 1991. Cerebral amyloid plaques in Alzheimer's disease but not in scrapie-affected mice are closely associated with a local inflammatory process. *Virchows Arch. B Cell Pathol. Incl. Mol. Pathol.* **60**: 329-336.

Ekeke G.I., and G.O. Ibeh, 1988, Sialic acid in sickle cell disease. *Clin Chem.* **34(7)**:1443-6.

Elmariah S.B., M.A. Crumling, T.D. Parsons, R.J. Balice-Gordon, 2004. Postsynaptic TrkB-mediated signaling modulates excitatory and inhibitory neurotransmitter receptor clustering at hippocampal synapses. *J Neurosci.* **24(10):** 2380-2393

Emsley J, H.E. White, B.P. O'Hara, G. Oliva, N. Srinivasan, I.J. Tickle, T.L. Blundell, M.B. Pepys, S.P. Wood, 1994. Structure of pentameric human serum amyloid P component. *Nature* **367(6461):**338-345

Ferrari,G. and L.A.Greene. 1998. Promotion of Neuronal Survival by GM1 Ganglioside: Phenomenology and Mechanism of Action. *Ann N Y Acad Sci* **19**: pp. 263-273.

Fink,M., F.Duprat, F.Lesage, R.Reyes, G.Romey, C.Heurteaux, M.Lazdunski. 1996. Cloning, functional expression and brain localization of a novel unconventional outward rectifier K+ channel. *EMBO J.* **15**: 6854-6862.

Flood D. G. and P.S. Coleman, 1990. Hippocampal plasticity in normal aging and decreased plasticity in Alzheimer's disease. *Prog. Brain Res.* **83**: 435–443.

Garofalo T., M. Sorice, R. Misasi, B. Cinque, V. Mattei, G.M. Pontieri, M.G. Cifone, A. Pavan, 2002. Ganglioside GM3 activates ERKs in human lymphocytic cells. *J Lipid Res* **43(6):** 971-978

Gouni-Berthold,I., C.Seul, Y.Ko, J.Hescheler, A.Sachinidis. 2001. Gangliosides GM1 and GM2 Induce Vascular Smooth Muscle Cell Proliferation via Extracellular Signal-Regulated Kinase 1/2 Pathway. *Hypertension* **38:** pp. 1030-1038

Gregorio-Rocasolano,N., T.Gasull, R.Trullas. 2001. Overexpression of neuronal pentraxin 1 is involved in neuronal death evoked by low K(+) in cerebellar granule cells. *J. Biol Chem.* **276**: 796-803

Griffin,W.S., L.C.Stanley, C.Ling, L.White, V.MacLeod, L.J.Perrot, C.L.White, C.Araoz. 1989. Brain interleukin 1 and S-100 immunoreactivity are elevated in Down syndrome and Alzheimer disease. *Proc Natl Acad Sci U S A* **86**: 7611-7615.

Hansson O., A. Petersen, M. Leist, P. Nicotera, R.F. Castilho, P. Brundin, 1999. Transgenic mice expressing a Huntington's disease mutation are resistant to quinolinic acid-induced striatal excitotoxicity. *Proc. Natl. Acad. Sci. U.S.A.* **96:** 8727–8732.

Hays S. J., 1998, Therapeutic approaches to the treatment of neuroinflammatory diseases. Curr. Pharm. Des **4**, 335–348.

Hering, H., C.C. Lin, M. Sheng, 2003. Lipid Rafts in the Maintenance of Synapses, Dendritic Spines, and Surface AMPA Receptor Stability. *J. Neurosci.* **23(8):** 3262–3271

Hetier,E., J.Ayala, P.Denefle, A.Bousseau, P.Rouget, M.Mallat, A.Prochiantz. 1988. Brain macrophages synthesize interleukin-1 and interleukin-1 mRNAs in vitro. *J. Neurosci. Res.* **21**: 391-397.

Higashi H., N.H. Chen, 2004. Ganglioside/protein kinase signals triggering cytoskeletal actin reorganization. *Glycoconj J* **20(1):** 49-58

Hirsch,E.C., S.Hunot, P.Damier, B.Faucheux. 1998. Glial cells and inflammation in Parkinson's disease: a role in neurodegeneration? *Ann. Neurol.* **44**: S115-S120.

Hossain,M.A., J.C.Russell, R.O'Brien, J. Laterra, 2004. Neuronal Pentraxin 1: A Novel Mediator of Hypoxic-Ischemic Injury in Neonatal Brain. *The Journal of Neuroscience*, **24**(17):4187-4196

Inokuchi,J., K. Kabayama, S. Uemura1 Y. Igarashi 2003. Glycosphingolipids govern gene expression. *Glycoconjugate Journal,* **20** (3): 169-178

Igdoura,S.A., C.Mertineit, J.M.Trasler, R.A.Gravel. 1999. Sialidase-mediated depletion of G_{M2} ganglioside in Tay-Sachs neuroglia cells. *Hum Mol Genet* **8(6)** pp. 1111-1116.

Jeyakumar,M., T.D.Butters, M.Cortina-Borja, V.Hunnam, R.L.Proia, V.H.Perry, R.A.Dwek, F.M.Platt. 1999. Delayed symptom onset and increased life expectancy in Sandhoff disease mice treated with N-butyldeoxynojirimycin. *Proc Natl Acad Sci U S A* **96**: 6388-6393.

Jeyakumar,M., R.Thomas, E.Elliot-Smith, D.A.Smith, A.C.van der Spoel, A.d'Azzo, V.H.Perry, T.D.Butters, R.A.Dwek, F.M.Platt. 2003. Central nervous system inflammation is a hallmark of pathogenesis in mouse models of GM1 and GM2 gangliosidosis. *Brain* **126**: 974-987.

Kanwar J.R., 2005. Anti-inflammatory immunotherapy for multiple sclerosis/experimental autoimmune encephalomyelitis (EAE) disease. *Curr Med Chem* **12(25):**2947-62

Karpas,A., G.W.Fleet, R.A.Dwek, S.Petursson, S.K.Namgoong, N.G.Ramsden, G.S.Jacob, T.W.Rademacher. 1988. Aminosugar derivatives as potential anti-human immunodeficiency virus agents. *Proc Natl Acad Sci U S A* **85**: 9229-9233.

Katoh N., T. Miyamoto, 1996. Enhancement by ganglioside GT1b of annexin I phosphorylation in bovine mammary gland in the presence of phosphatidylserine and Ca2+. *Lipids* **31(9):**983-987

Katoh,S., T.Miyagi, H.Taniguchi, Y.Matsubara, J.Kadota, A.Tominaga, P.W.Kincade, S.Matsukura, S.Kohno. 1999. Cutting edge: an inducible sialidase regulates the hyaluronic acid binding ability of CD44-bearing human monocytes. *J. Immunol.* **162**: 5058-5061.

Kerkut, G.A., S. Nicolaidis, S.M. Piggott, C.G. Rasool, R.J. Walker, 1974. Proceedings: The effect of analogues of glutamic acid on the glutamate receptors of Helix neurones. *Br J Pharmacol.* 51(1):134P-135P

Kim G. M., J. Xu, J.M. Xu, S.K. Song, P. Yan, G. Ku, X.M. Xu, C.Y. Hsu, 2001, Tumor necrosis factor receptor deletion reduces nuclear factor-kappa B activation, cellular inhibitor of apoptosis protein 2 expression, and functional recovery after traumatic spinal cord injury. J. Neurosci. **21**, 6617–6625.

King A.E., R.S. Chung, J.C. Vickers, T.C. Dickson, 2006. Localization of glutamate receptors in developing cortical neurons in culture and relationship to susceptibility to excitotoxicity. *J Comp Neurol.* **498(2)**:277-94.

Klampfer, L, J. Huang, L. A. Swaby, L. Augenlicht, 2004. Requirement of Histone Deacetylase Activity for Signaling by STAT1. *J. Biol. Chem* **279 (29)** 30358-30368

Levine M. S., G.J. Klapstein, A. Koppel, 1999. Enhanced sensitivity to N-methyl-D-aspartate receptor activation in transgenic and knockin mouse models of Huntington's disease. *J. Neurosci. Res.* **58:** 515–532.

Li R, Y. Liu, S. Ladisch, 2001. Enhancement of epidermal growth factor signaling and activation of SRC kinase by gangliosides. *J Biol Chem* **276:** 42782–92

Liu J.R., M.P. Ding, E.Q. Wei, J.H. Luo, Y. Song, J.Z. Huang , Q.F. Ge, H. Hu, L.J. Zhu, 2005. GM1 stabilizes expression of NMDA receptor subunit 1 in the ischemic hemisphere of MCAo/reperfusion rat. *J Zhejiang Univ Sci B.* **6**(4):254-258

Lo, E.H., A.R. Pierce, J.B. Mandeville, B.R. Rosen, 1997. Neuroprotection With NBQX in Rat Focal Cerebral Ischemia Effects on ADC Probability Distribution Functions and Diffusion-Perfusion Relationships *Stroke* **28:** 439-447

Luthi-Carter R., B.L. Apostol, A.W. Dunah, M.M. DeJohn, L.A. Farrell, G.P. Bates, A.B. Young, D.G. Standaert, L.M. Thompson, J.H. Cha, 2003. Complex alteration of NMDA receptors in transgenic Huntington's disease mouse brain: analysis of mRNA and protein expression, plasma membrane association, interacting proteins, and phosphorylation. *Neurobiol. Dis.* **14:** 624–636.

Marmillot P, M.N. Rao, Q.H. Liu, M.R. Lakshman, 1999, Desialylation of human apolipoprotein E decreases its binding to human high-density lipoprotein and its ability to deliver esterified cholesterol to the liver. *Metabolism* **48(9)**:1184-92

Masserini M., M. Pitto, A. Ferraretto, J. Brunne, P. Palestini, 1998. Glycolipid-protein interaction in the mechanism of signal transduction: studies with a photoactivable ganglioside analogue. *Acta Biochim Pol* **45(2):** 393-401

Menzies-Gow A., S. Ying, I. Sabroe, V.L. Stubbs, D. Soler, T.J. Williams, A.B. Kay, 2002 Eotaxin (CCL11) and eotaxin-2 (CCL24) induce recruitment of eosinophils, basophils, neutrophils, and macrophages as well as features of early- and late-phase allergic reactions following cutaneous injection in human atopic and nonatopic volunteers. *J Immunol.* **169(5)**:2712-8

Miljan E.A., E.J. Meuillet, B. Mania-Farnell, D. George, H. Yamamoto, H.G. Simon, E.G. Bremer, 2002. Interaction of the extracellular domain of the epidermal growth factor receptor with gangliosides. *J Biol Chem* **277:** 10108–13

Min K.J., M.S. Yang, I. Jou, E.H. Joe, 2004. Protein kinase A mediates microglial activation induced by plasminogen and gangliosides. *Exp Mol Med* **36(5):**461-467

Minghetti L., M.A. Ajmone-Cat, M.A. De Berardinis, R. De Simone, 2005, Microglial activation in chronic neurodegenerative diseases: roles of apoptotic neurons and chronic stimulation. *Brain Res. Rev.* **48**, 251–256.

Mutoh T, A. Tokuda, T. Miyadai, M. Hamaguchi, N. Fujiki, 1995. Ganglioside GM1 binds to the Trk protein and regulates receptor function. *Proc Natl Acad Sci U S A* **92(11):**5087-5091

Myerowitz,R., H.Mizukami, K.L.Richardson, L.S.Finn, C.J.Tifft, R.L.Proia. 2004. Global gene expression in a type 2 Gaucher disease brain. *Mol. Genet. Metab* **83**: 288-296.

Noda M., H. Kettenmann, K. Wada, 2006, Anti-inflammatory effects of kinins via microglia in the central nervous system. *Biol. Chem.* **387**, 167–171.

O'Brien R.J., L.F. Lau, R.L. Huganir, 1998. Molecular mechanisms of glutamate receptor clustering at excitatory synapses. *Curr Opin Neurobiol* **8(3):** 364-369

Orozco-Ibarra M, Y.I. Chirino, J. Pedraz -Chaverri, 2006. Role of hemeoxygenase-1 in the neurodegenerative disorders. *Rev Neurol* **43(9)**:556-62

Palestini P, M. Pitto, A. Ferraretto, G. Tettamanti, M. Masserini, 1998. Change of ganglioside accessibility at the plasma membrane surface of cultured neurons, following protein kinase C activation. *Biochemistry* **37(9):**3143-3148

Pettus B.J., C.E. Chalfant, Y.A. Hannun 2002. Ceramide in apoptosis: an overview and current perspectives. *Biochim Biophys Acta.* **1585(2-3)**:114-25

Phaneuf,D., N.Wakamatsu, J.-Q.Huang, A.Borowski, A.C.Peterson, S.R.Fortunato, G.Ritter, S.A.Igdoura, C.R.Morales, G.Benoit, B.R.Akerman, D.Leclerc, N.Hanai, J.D.Marth, J.M.Trasler, R.A.Gravel. 1996. Dramatically different phenotypes in mouse models of human Tay-Sachs and Sandhoff diseases. *Hum. Mol Genet* **5** pp. 1-14.

Pelled, D., H. Shogomori, A.H. Futerman, 2000. The increased sensitivity of neurons with elevated glucocerebroside to neurotoxic agents can be reversed by imiglucerase. *Journal of Inherited Metabolic Disease* **23:** 175–184.

Platt,F.M., G.R.Neises, R.A.Dwek, T.D.Butters. 1994. N-butyldeoxynojirimycin is a novel inhibitor of glycolipid biosynthesis. *J. Biol Chem.* **269**: 8362-8365.

Platt,F.M., G.R.Neises, G.Reinkensmeier, M.J.Townsend, V.H.Perry, R.L.Proia, B.Winchester, R.A.Dwek, T.D.Butters. 1997. Prevention of lysosomal storage in Tay-Sachs mice treated with N-butyldeoxynojirimycin. *Science* **276**: 428-431.

Platt,F.M. T.D.Butters. 2000. Substrate deprivation: A new therapeutic approach for the glycosphingolipid lysosomal storage diseases. *Expert Rev Mol Med.* **1**;2000:1-17.

Rahmann H., F. Schifferer, H. Beitinger, 1992. Calcium-ganglioside interactions and synaptic plasticity: effect of calcium on specific ganglioside/peptide (valinomycin, gramicidin A)-complexes in mixed mono- and bilayers. *Neurochem Int* **20(3):**323-338

Rampersaud A.A., J.L. Oblinger, R.K. Ponnappan, R.W. Burry, A.J. Yates, 1999. Gangliosides and growth factor receptor regulation. *Biochem Soc Trans.* **27(4):**415-22

Riboni,L., A.Caminiti, R.Bassi, G.Tettamanti. 2004. The Degradative Pathway of Gangliosides GMI and GM2 in Neurola Cells by Sialidase. *J. Neurochem.* **64(1)** pp. 451-454.

Rosenberg L.J., Y.D. Teng, J.R. Wrathall 1999. 2,3-Dihydroxy-6-Nitro-7-Sulfamoyl-Benzo(f)Quinoxaline Reduces Glial Loss and Acute White Matter Pathology after Experimental Spinal Cord Contusion *The Journal of Neuroscience* **19(1):**464-475

Rubinsztein D. C., J. Leggo, M. Chiano, A. Dodge, G. Norbury, E. Rosser, D. Craufurd, 1997. Genotypes at the GluR6 kainate receptor locus are associated with variation in the age of onset of Huntington disease. *Proc. Natl. Acad. Sci. U.S.A.* **94:** 3872–3876.

de Ruiter J. P. and H.B. Uylings, 1987. Morphometric and dendritic analysis of fascia dentata granule cells in human aging and senile dementia. *Brain Res.* **402**: 217–229.

Sango,K., S.Yamanaka1, A.Hoffmann, Y.Okuda, A.Grinberg, H.Westphal, M.P.McDonald, J.N.Crawley, K.Sandhoff, K.Suzuki, R.L.Proia. 1995. Mouse models of Tay–Sachs and Sandhoff diseases differ in neurologic phenotype and ganglioside metabolism. *Nat Genet* **11(2)** pp. 170-176.

Small D. H., S.S. Mok, J.C. Bornstein, 2001. Alzheimer's disease and Abeta toxicity: from top to bottom. *Nat. Rev. Neurosci.* **2:** 595–598.

Smith, C.P., S. Weremowicz, Y. Kanai, M. Stelzner , C.C. Morton, M.A. Hediger. 1994. Assignment of the gene coding for the human high-affinity glutamate transporter EAAC1 to 9p24: potential role in dicarboxylic aminoaciduria and neurodegenerative disorders. *Genomics* **20(2)**: pp. 335-336.

Snyder E. M., Y. Nong, C.G. Almeida, 2005 Regulation of NMDA receptor trafficking by amyloid-beta. *Nat. Neurosci.* **8:**1051–1058.

Sokka A.L., N. Putkonen, G. Mudo, E. Pryazhnikov, S. Reijonen, L. Khiroug, N. Belluardo, D. Lindholm, L. Korhonen, 2007. Endoplasmic reticulum stress inhibition protects against excitotoxic neuronal injury in the rat brain. *J Neurosci.* **27(4)**: 901-908.

Sonnino S., V. Chigorno, M. Valsecchi, M. Pitto, G. Tettamanti, 1992. Specific ganglioside-cell protein interactions: a study performed with GM1 ganglioside derivative containing photoactivable azide and rat cerebellar granule cells in culture. *Neurochem Int* **(3):**315-321

Spiegel,S., D.Foster, R.Kolesnick. 1996. Signal transduction through lipid second messengers. *Curr Opin Cell Biol* **8(2)** pp. 159-167.

Stamatos,N.M., S.Curreli, D.Zella, A.S.Cross. 2003. Desialylation of glycoconjugates on the surface of monocytes activates the extracellular signal-related kinases ERK 1/2 and results in enhanced production of specific cytokines. *J. Leuk Biol.***75:** 307-313.

Stern E. A., B.J. Bacskai, G.A. Hickey, F.J. Attenello, J.A. Lombardo, B.T. Hyman, 2004. Cortical synaptic integration in vivo is disrupted by amyloid-beta plaques. *J. Neurosci.* **24:** 4535–4540.

Suchi,M., T.Dinur, R.J.Desnick, S.Gatt, L.Pereira, E.Gilboa, E.H.Schuchman. 1992. Retroviral-mediated transfer of the human acid sphingomyelinase cDNA: correction of the metabolic defect in cultured Niemann-Pick disease cells. *Proc Natl Acad Sci U S A* **89**: 3227-3231.

Sun D., T.A. Newman, V.H. Perry, R.O. Weller, 2004, Cytokine induced enhancement of autoimmune inflammation in the brain and spinal cord: implications for multiple sclerosis. *Neuropathol. Appl. Neurobiol.* **30**, 374–384.

Sun Y., A. Savanenin, P.H. Reddy, Y.F. Liu, 2001. Polyglutamineexpanded huntingtin promotes sensitization of N-methyl-D-aspartate receptors via post-synaptic density. *J. Biol. Chem.* **276:** 24713–24718.

Susuki,K., M.N. Rasband, K. Tohyama, K. Koibuchi, S. Okamoto, K. Funakoshi, K. Hirata, H. Baba, N. Yuki, 2007. Anti-GM1 Antibodies Cause Complement-Mediated Disruption of Sodium Channel Clusters in Peripheral Motor Nerve Fibers. *J Neurosci.* **27**:3956 –3967

Suzuki, T. , J. Itob, H. Takagia, F. Saitoha, H. Nawac, H. Shimizu, 2001. Biochemical evidence for localization of AMPA-type glutamate receptor subunits in the dendritic raft *Molecular Brain Research* **89**: 20–28

Taki,T., Y.Hirabayashi, K.Takagi, R.Kamada, K.Kojima, M.Matsumoto. 1981. Purification of anti-glycosphingolipid antibody and topological localization of glycosphingolipid on the cell surface of rat ascites hepatomas. *J. Biochem* **89(2)** pp. 503-510.

Takigawa T, H. Yasuda, 1995. The effect of anti-GM1 antibodies on ionic channel in myelinated nerve. *Rinsho Shinkeigaku* **35(12):**1377

Toledo M.S., E. Suzuki, K. Handa, S. Hakomori, 2005. Effect of ganglioside and tetraspanins in microdomains on interaction of integrins with fibroblast growth factor receptor. *J Biol Chem* **280(16):**16227-16234

Tsui C.C., N.G. Copeland, D.J. Gilbert, N.A. Jenkins, C. Barnes, P.F. Worley, 1996. Narp, a novel member of the pentraxin family, promotes neurite outgrowth and is dynamically regulated by neuronal activity. *J Neurosci* **16(8):** 2463-2478

Vaccarino F, A. Guidotti A, E. Costa, 1987. Ganglioside inhibition of glutamate-mediated protein kinase C translocation in primary cultures of cerebellar neurons. *Proc Natl Acad Sci U S A* **84(23):** 8707-8711

Walkley,S.U., D.A.Segel, K.Dobrenis, Zervas.Mark. 1998. GM2 Ganglioside as a Regulator of Pyramidal Neuron Dendritogenesis. *Ann N Y Acad Sci* **845** pp. 188-199.

Wallace, J.L., 1999. Distribution and expression of cyclooxygenase (COX) isoenzymes, their physiological roles, and the categorization of nonsteroidal anti-inflammatory drugs (NSAIDs). *Am. J. Med.* **107(6A):**11S-16S

Wu D. and S. N. Meydani, 1998, n-3 polyunsaturated fatty acids and immune function. *Proc. Nutr. Soc.* 57, 503–509.

Xuesong C, S. Chi, M. Liu, W. Yang, T. Wei, Z. Qi, F. Yang, 2005. Inhibitory effect of ganglioside GD1b on K+ current in hippocampal neurons and its involvement in cell apoptosis suppression. *Journal of Lipid Research* **46:** 2580-2585

Yada Y, Y. Okano, Y. Nozawa, 1991. Ganglioside GQ1b-induced terminal differentiation in cultured mouse keratinocytes. Phosphoinositide turnover forms the onset signal. *Biochem J* **279:**665-670

Yam,G.H., N.Bosshard, C.Zuber, B.Steinmann, J.Roth. 2006. Pharmacological chaperone corrects lysosomal storage in Fabry disease caused by trafficking-incompetent variants. *Am. J. Physiol Cell Physiol* **290**: C1076-C1082.

Zerangue N. and M.P. Kavanaugh, 1996. Interaction of 1-cysteine with a human excitatory amino acid transporter. *J. Physiol.* **493**: 419–423.

Zervas,M., K.L.Somers, M.A.Thrall, S.U.Walkley. 2001. Critical role for glycosphingolipids in Niemann-Pick disease type C. *Curr Biol* **11**: 1283-1287.

Appendix A: Classification of genes altered in Tay Sachs neuroglia

Figure A-1: A comparison of gene expressions in human microglia cells. The fist column is the number of genes from the array that are present in the corresponding pathway. The second column is the total percent of significantly altered genes in the pathway. Only those genes with at least a twofold change were recorded. A) Up regulated genes in microglia from a Tay Sachs patient compared to those of a normal patient. B) Down regulated genes in microglia from a Tay Sachs patient compared to those of a normal patient. A list of genes and their corresponding relative expression levels were inputted into the Onto Express software.

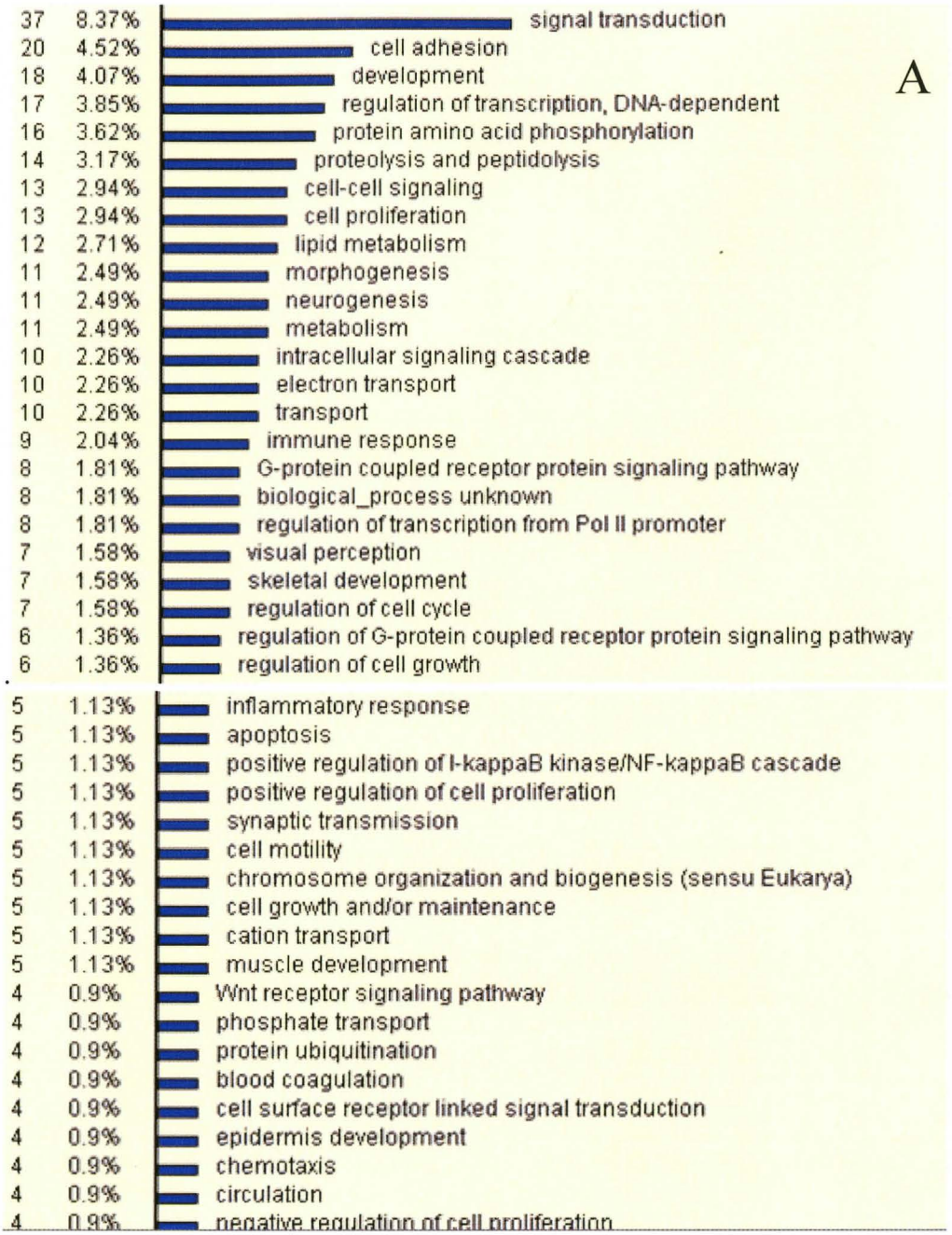
37 8.37% signal transduction
20 4.52% cell adhesion
18 4.07% development
17 3.85% regulation of transcription, DNA-dependent
16 3.62% protein amino acid phosphorylation
14 3.17% proteolysis and peptidolysis
13 2.94% cell-cell signaling
13 2.94% cell proliferation
12 2.71% lipid metabolism
11 2.49% morphogenesis
11 2.49% neurogenesis
11 2.49% metabolism
10 2.26% intracellular signaling cascade
10 2.26% electron transport
10 2.26% transport
9 2.04% immune response
8 1.81% G-protein coupled receptor protein signaling pathway
8 1.81% biological_process unknown
8 1.81% regulation of transcription from Pol II promoter
7 1.58% visual perception
7 1.58% skeletal development
7 1.58% regulation of cell cycle
6 1.36% regulation of G-protein coupled receptor protein signaling pathway
6 1.36% regulation of cell growth
5 1.13% inflammatory response
5 1.13% apoptosis
5 1.13% positive regulation of I-kappaB kinase/NF-kappaB cascade
5 1.13% positive regulation of cell proliferation
5 1.13% synaptic transmission
5 1.13% cell motility
5 1.13% chromosome organization and biogenesis (sensu Eukarya)
5 1.13% cell growth and/or maintenance
5 1.13% cation transport
5 1.13% muscle development
4 0.9% Wnt receptor signaling pathway
4 0.9% phosphate transport
4 0.9% protein ubiquitination
4 0.9% blood coagulation
4 0.9% cell surface receptor linked signal transduction
4 0.9% epidermis development
4 0.9% chemotaxis
4 0.9% circulation
4 0.9% negative regulation of cell proliferation

A

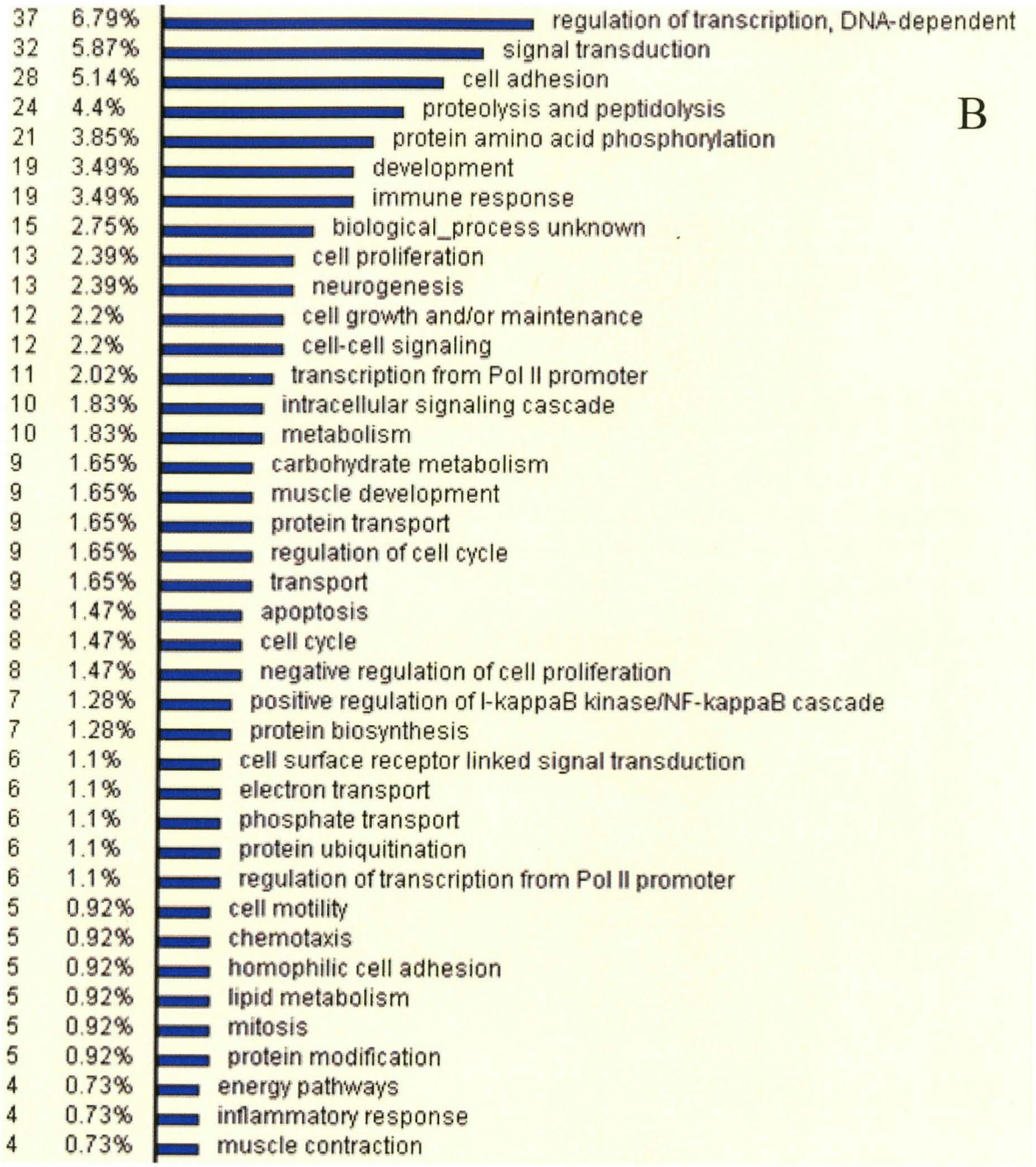
37 6.79% regulation of transcription, DNA-dependent
32 5.87% signal transduction
28 5.14% cell adhesion
24 4.4% proteolysis and peptidolysis
21 3.85% protein amino acid phosphorylation
19 3.49% development
19 3.49% immune response
15 2.75% biological_process unknown
13 2.39% cell proliferation
13 2.39% neurogenesis
12 2.2% cell growth and/or maintenance
12 2.2% cell-cell signaling
11 2.02% transcription from Pol II promoter
10 1.83% intracellular signaling cascade
10 1.83% metabolism
9 1.65% carbohydrate metabolism
9 1.65% muscle development
9 1.65% protein transport
9 1.65% regulation of cell cycle
9 1.65% transport
8 1.47% apoptosis
8 1.47% cell cycle
8 1.47% negative regulation of cell proliferation
7 1.28% positive regulation of I-kappaB kinase/NF-kappaB cascade
7 1.28% protein biosynthesis
6 1.1% cell surface receptor linked signal transduction
6 1.1% electron transport
6 1.1% phosphate transport
6 1.1% protein ubiquitination
6 1.1% regulation of transcription from Pol II promoter
5 0.92% cell motility
5 0.92% chemotaxis
5 0.92% homophilic cell adhesion
5 0.92% lipid metabolism
5 0.92% mitosis
5 0.92% protein modification
4 0.73% energy pathways
4 0.73% inflammatory response
4 0.73% muscle contraction
B

Table A-1: Pathways altered between Tay Sachs and Normal neuroglia cells grouped by PANTHER gene expression analysis. Only those genes with at least a twofold change were recorded. The software offered a visual analysis of the pathways altered. Visual representations of pathways that may be relevant to the disease are present in figure A-2.

Angiogenesis	13
Inflammation mediated by chemokine and cytokine signaling pathway	12
Wnt signaling pathway	12
Heterotrimeric G-protein signaling pathway-Gi alpha and Gs alpha mediated pathway	8
Integrin signalling pathway	7
Heterotrimeric G-protein signaling pathway-Gq alpha and Go alpha mediated pathway	7
Cadherin signaling pathway	6
TGF-beta signaling pathway	5
Alzheimer disease-presenilin pathway	4
Interleukin signaling pathway	4
FGF signaling pathway	4
EGF receptor signaling pathway	4
Oxidative stress response	4
Metabotropic glutamate receptor group III pathway	3
5HT2 type receptor mediated signaling pathway	3
Huntington disease	3
Endothelin signaling pathway	3
PI3 kinase pathway	3
Blood coagulation	3
Metabotropic glutamate receptor group II pathway	3
Axon guidance mediated by Slit/Robo	2
Ionotropic glutamate receptor pathway	2
Alpha adrenergic receptor signaling pathway	2
Insulin/IGF pathway-protein kinase B signaling cascade	2
p53 pathway	2
Plasminogen activating cascade	2
Nicotinic acetylcholine receptor signaling pathway	2
D2/D3/D4 dopamine receptor mediated signaling pathway	2
Muscarinic acetylcholine receptor 2 and 4 signaling pathway	2
D1/D5 dopamine receptor mediated sigaling pathway	2
Muscarinic acetylcholine receptor 1 and 3 signaling pathway	2
Metabotropic glutamate receptor group I pathway	2

Figure A-2:

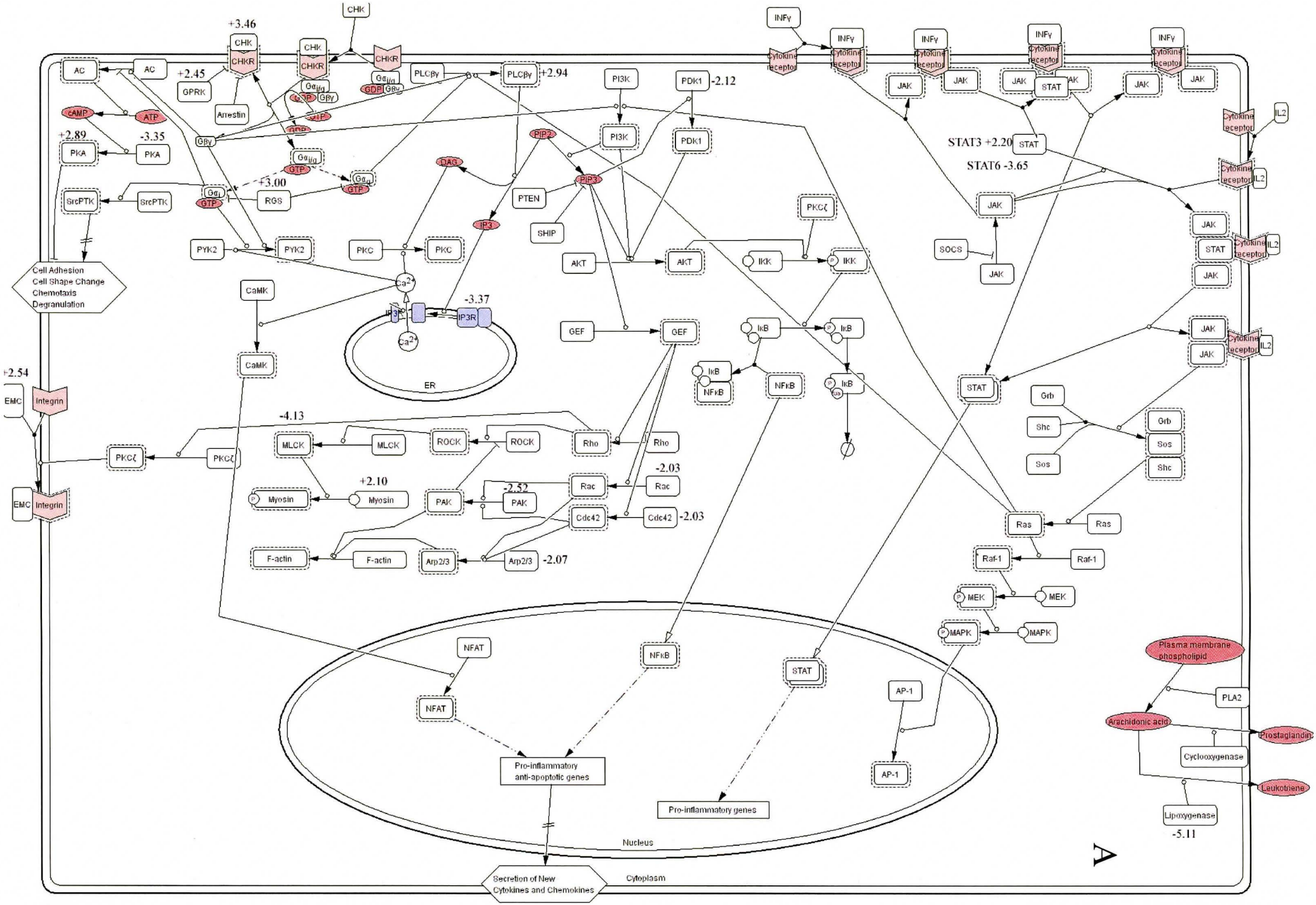
+3.46
CHK
CHKR
+2.45
GPRK
Arrestin
AC
cAMP
ATP
+2.89
PKA
-3.35
PKA
SrcPTK
+3.00
RGS
PLCβγ
+2.94
PI3K
PDK1
-2.12
PIP2
PIP3
PTEN
SHIP
DAG
IP3
PYK2
PKC
Ca2+
ER
-3.37
IP3R
CaMK
GEF
IkB
NFkB
AKT
IKK
PKCζ
Cell Adhesion
Cell Shape Change
Chemotaxis
Degranulation
+2.54
EMC
Integrin
-4.13
MLCK
ROCK
Rho
-2.03
Rac
Cdc42
PAK
-2.52
+2.10
Myosin
F-actin
Arp2/3
-2.07
INFγ
Cytokine receptor
JAK
STAT
STAT3 +2.20
STAT6 -3.65
SOCS
IL2
Grb
Shc
Sos
Ras
Raf-1
MEK
MAPK
NFAT
NFκB
AP-1
Pro-inflammatory anti-apoptotic genes
Pro-inflammatory genes
Nucleus
Secretion of New Cytokines and Chemokines
Cytoplasm
Plasma membrane phospholipid
PLA2
Arachidonic acid
Prostaglandin
Cyclooxygenase
Leukotriene
Lipoxygenase
-5.11
A

B

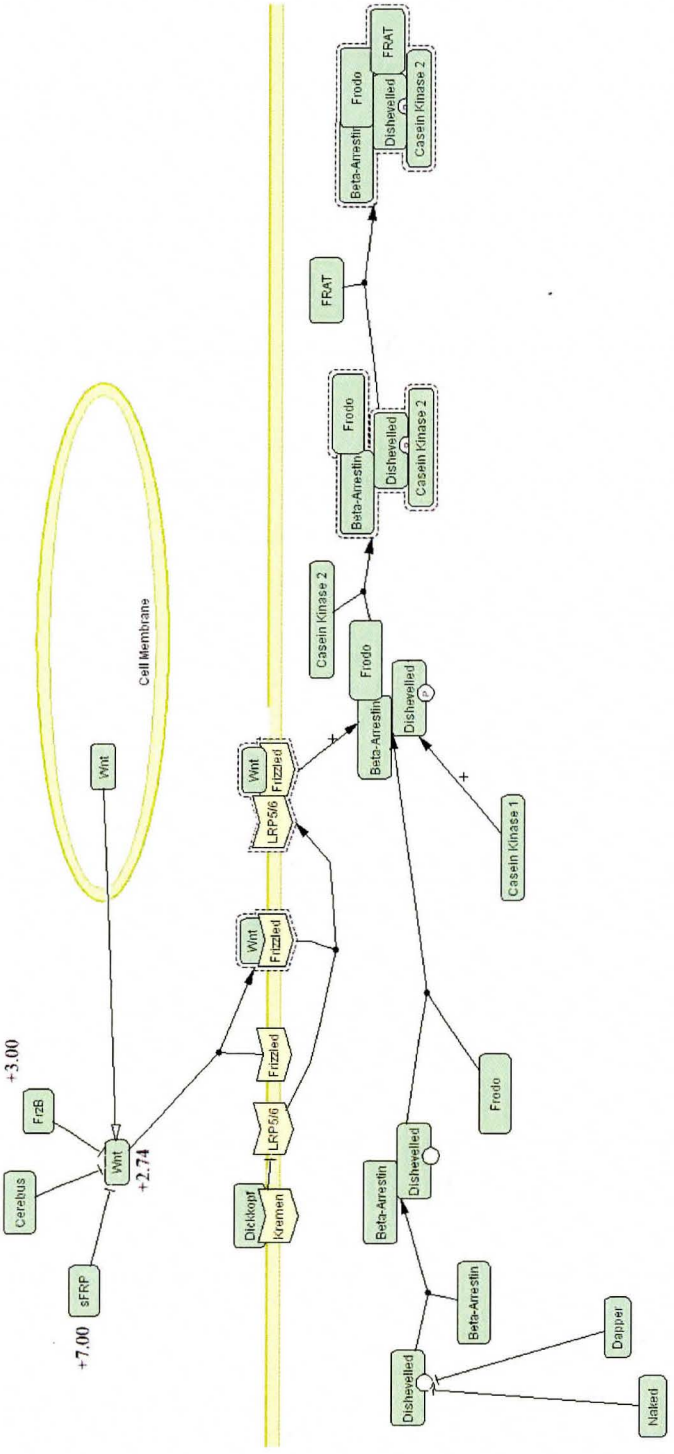
Cell Membrane
Wnt
Fz8
Cerebus
sFRP
+3.00
+7.00
+2.74
Frizzled
LRP5/6
Dickkopf
Kremen
Beta-Arrestin
Dishevelled
Frodo
Casein Kinase 2
Casein Kinase 1
FRAT
Dapper
Naked

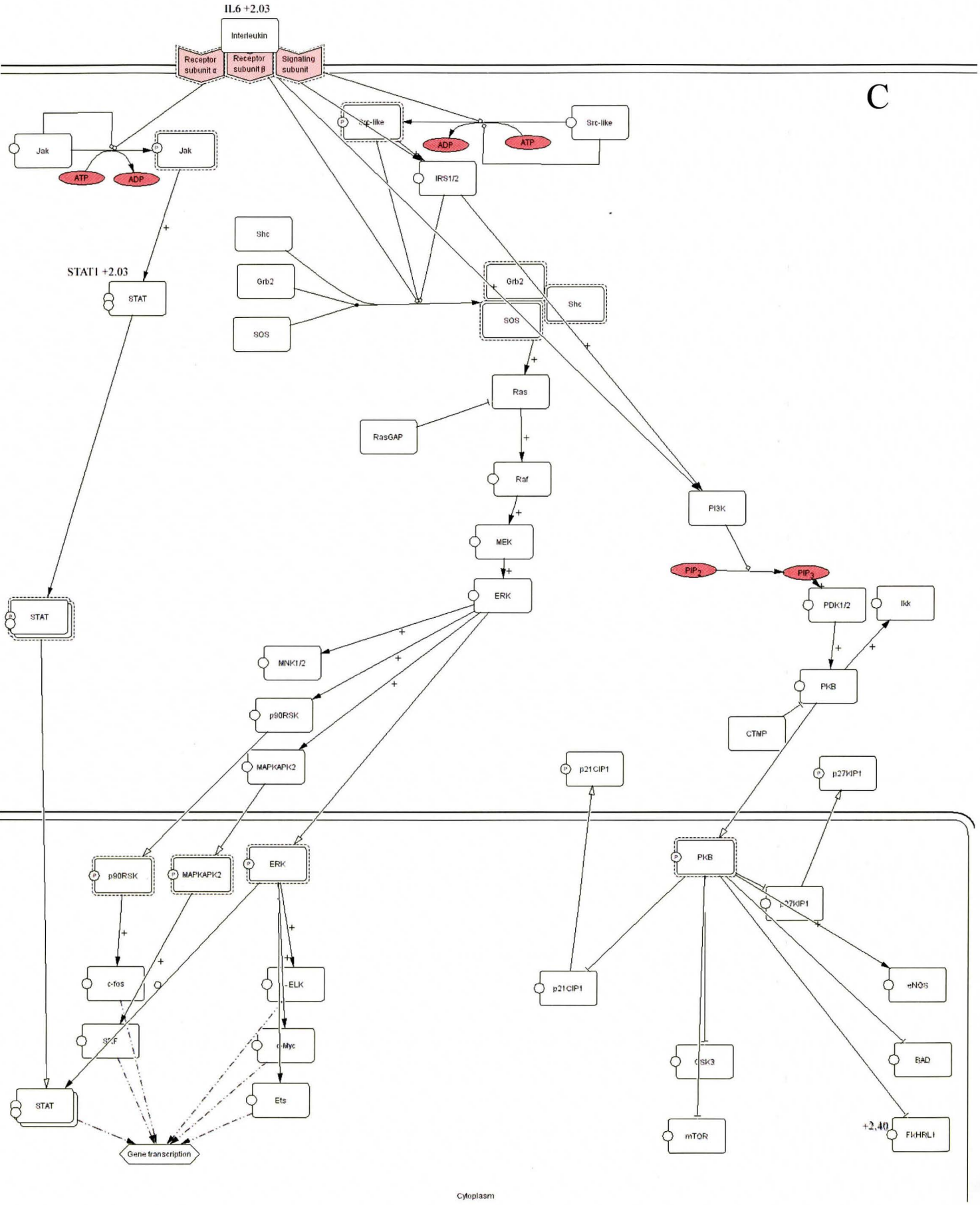
IL6 +2.03
Interleukin
Receptor subunit α
Receptor subunit β
Signaling subunit
C
Jak
Jak
ATP
ADP
Src-like
Src-like
ADP
ATP
IRS1/2
Shc
Grb2
SOS
Grb2
Shc
SOS
STAT1 +2.03
STAT
Ras
RasGAP
Raf
MEK
ERK
PI3K
PIP2
PIP3
PDK1/2
Ikk
PKB
CTMP
MNK1/2
p90RSK
MAPKAPK2
p21CIP1
p27KIP1
STAT
p90RSK
MAPKAPK2
ERK
PKB
p27KIP1
c-fos
c-ELK
p21CIP1
eNOS
SRF
c-Myc
GSK3
BAD
STAT
Ets
mTOR
+2.40
FKHRL1
Gene transcription
Cytoplasm

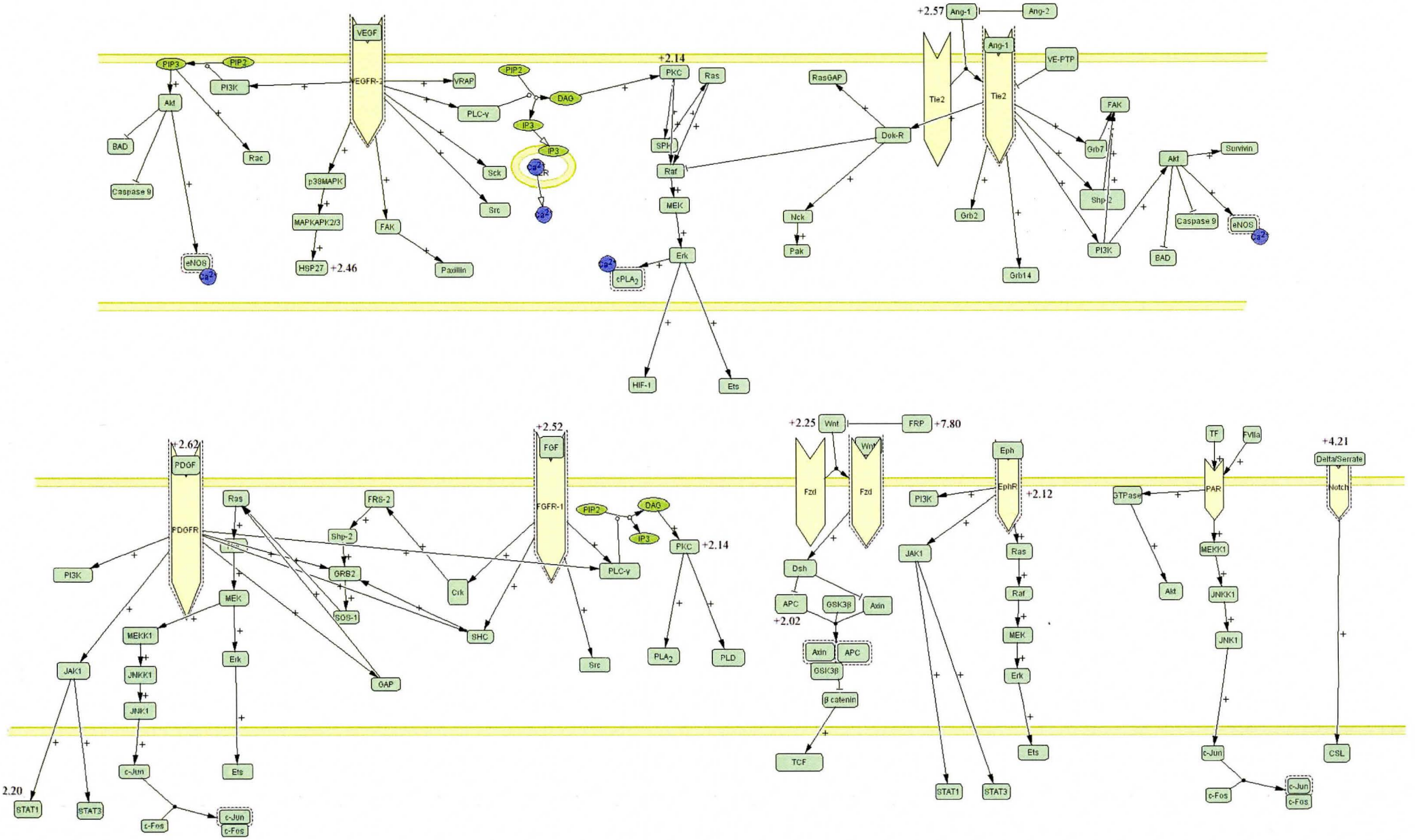
VEGF
VEGFR-2
PIP3
PIP2
PI3K
Akt
BAD
Caspase 9
Rac
eNOS
Ca2+
p38MAPK
MAPKAPK2/3
HSP27
+2.46
FAK
Paxillin
Sck
Src
VRAP
PLC-γ
PIP2
DAG
IP3
IP3R
Ca2+
+2.14
PKC
Ras
SPK
Raf
MEK
Erk
cPLA2
HIF-1
Ets
+2.57
Ang-1
Ang-2
RasGAP
Tie2
Dok-R
Nck
Pak
Grb2
Grb14
VE-PTP
FAK
Grb7
Shp-2
PI3K
Akt
Survivin
Caspase 9
eNOS
BAD
+2.62
PDGF
PDGFR
Ras
FRS-2
Shp-2
GRB2
SOS-1
Crk
SHC
GAP
PI3K
MEK
MEKK1
JNKK1
JNK1
JAK1
Erk
c-Jun
c-Fos
Ets
2.20
STAT1
STAT3
+2.52
FGF
FGFR-1
PIP2
DAG
IP3
PKC
+2.14
PLC-γ
Src
PLA2
PLD
+2.25
Wnt
FRP
+7.80
Fzd
Dsh
APC
GSK3β
Axin
+2.02
β catenin
TCF
Eph
EphR
+2.12
PI3K
JAK1
Ras
Raf
MEK
Erk
Ets
STAT1
STAT3
TF
FVIIa
GTPase
PAR
Akt
MEKK1
JNKK1
JNK1
c-Jun
c-Fos
+4.21
Delta/Serrate
Notch
CSL

D

Table 1: Genes selected for confirmation via Real Time PCR. Genes were selected based on their appearance in the pathways in appendices A, B, C, and table A-1 (IL6, PLCB4, ITPR3, PTGS1, CASP1, HDAC1, SMPD1, CAPN1, and ITPR3), if there were extreme differences between the normal and Tay Sach's cells (CCL11, NPTX1, HMOX1, KCNK2). A negative fold difference indicates a reduction of the gene in Tay Sach's cells while a positive number is indicative of an increase. The biological involvement of the genes was also a factor in their selection. CASP1, PTGS1, CCL11, AND IL6 are involved in inflammation; CAPN1 and ITPR3 are involved in calcium homeostasis; NPTX1 is involved in apoptosis mediated by potassium depletion and KNCK2 is a potassium channel that transports ions out of the cell.

GENE	Abbreviation	Biological Involvement	fold difference in Tay Sachs Cells
Caspase 1	CASP1	Inflammatory caspase; activator of Interleukin 1. The role of interleukin 1 has been depicted in other neurological diseases such as Alzheimer's as Down's Syndrome (Griffin et al., 1989). 2) Stimulation of microglia with LPS induces IL-1 (Hetier et al., 1988). 3) Data from the microarray reveals a massive upregulation of Caspase 1 in microglia from a Tay Sachs patient.	+12.98
Interleukin 6	IL6	Inflammatory cytokine, activates transcription of STAT1. activated by caspase 1.	+2.03
Heme Oxygenease 1	HMOX1	inhibition of heme oxygenase may result in increased oxidative neurotoxicity in AD, and has been shown to inhibit proinflammatory function; downregulated in Gaucher brain	-9.51
Histone Deacetlyase 1	HDAC1	involved in IFNgamma signaling via STAT1	-4.74
Potassium Channel, Subfamily K, Member 2	KCNK2	Potassium Channel. Responsible for leakage of potassium to extracellular space (Fink et al., 1996).	+7.82
Eotaxin	CCL11	Chemokine involved in	+20.41

		eosinophil recruitment.	
Neuronal Pentraxin 1	NPTX1	involved in apoptosis mediated by potassium deprivation(Gregorio-Rocasolano et al., 2001); upregulated in the brain of Gaucher patients(Myerowitz et al., 2004).	+20.52
Sphingomyelin Phosphodiesterase 1	SMPD1	synthesizes ceramide from sphingomyelin to inhibit apoptosis (Suchi et al., 1992).	-4.51
Phospholipase C, Beta-4	PLCB4	synthesizes inositol triphosphate (IP3) involved in intracellular signal transduction	+2.94
Calpain 1	CAPN1	induced in ER-stress mediated apoptosis	-2.89
Inositol 1,4,5-Triphosphate Receptor, Type 3	ITPR3	ITPR3 transduces many hormonal signals that regulate Ca(2+)-dependent processes	-3.37
Prostaglandin Synthase 1	PTGS1	Synthesizes prostaglandins leading to inflammation response	+6.50